Marine Pollution Bulletin 221 (2025) 118490

Contents lists available at ScienceDirect

Marine Pollution Bulletin

journal homepage: www.elsevier.com/locate/marpolbul

What do emerging PFAS tell us that the classic ones did not? Insights from *in vitro* assays

Marta Cunha [a,b], Claudio Bortot [c], Gianfranco Santovito [c], Alessandro Nardi [d,e], Amadeu M.V.M. Soares [a,b], Ana M. Gil [f], Rosa Freitas [a,b,*]

[a] Department of Biology, University of Aveiro, 3810-193 Aveiro, Portugal
[b] Centre for Environmental and Marine Studies (CESAM), University of Aveiro, 3810-193 Aveiro, Portugal
[c] Department of Biology, University of Padova, Italy
[d] Dipartimento di Scienze della Vita e dell'Ambiente, Università Politecnica delle Marche, Ancona, Italy
[e] NBFC, National Biodiversity Future Center, Palermo 90131, Italy
[f] CICECO — Aveiro Institute of Materials, Department of Chemistry, University of Aveiro, 3810-193 Aveiro, Portugal

ARTICLE INFO

Keywords:
PFAS
Bivalves
S9 sub-cellular fractions
Short exposure
Oxidative stress

ABSTRACT

Per- and polyfluoroalkyl substances (PFAS) are synthetic chemicals that are recognized for their environmental persistence and potential toxicity. As regulatory pressure increases on legacy PFAS, emerging alternatives are being increasingly used. However, their environmental toxicological profiles remain poorly understood. The present study compares the biochemical effects of legacy (PFOS, PFOA, and PFNA) and emerging (GenX, PFBA, PFBS, and PFHxS) PFAS on the mussel species *Mytilus galloprovincialis,* using *in vitro* exposures of digestive gland (DG) and gills (G) tissues. The results highlighted tissue-specific responses, with greater biochemical variability observed in the DG. This was particularly evident under exposure to emerging PFAS, which appeared to induce oxidative stress disturbances and detoxification pathways, as indicated by increased acetylcholinesterase (AChE) and glutathione S-transferases activities and reduced total antioxidant capacity (TAC) levels. In contrast, the G showed a strong inhibition of both AChE and carboxylesterases activities and decreased TAC levels, possibly due to neurotoxic effects and compromised redox homeostasis. These findings suggest that emerging PFAS induce diverse and pronounced effects in the DG, whereas legacy PFAS generally cause less divergent biochemical responses. Further research into intra-group variability, especially among emerging PFAS, is essential for understanding their ecological risks and developing targeted regulatory frameworks.

1. Introduction

In recent years, growing recognition within the scientific and public health communities has highlighted the widespread environmental contamination caused by synthetic chemicals (Li et al., 2024). *Per-* and polyfluoroalkyl substances (PFAS) are among the most concerning substances, comprising a large group of 15,000 human-made chemicals (USEPA, 2022) that have been detected worldwide in water (Crone et al., 2019; Kurwadkar et al., 2022), soil (Brusseau et al., 2020; Brusseau and Guo, 2022), wildlife (Bangma et al., 2022; Evich et al., 2025), and even human blood (Bangma et al., 2022; Göckener et al., 2020; Poothong et al., 2020). These substances are synthetic organofluorine compounds characterized by carbon chains in which all (perfluoroalkyl) or some (polyfluoroalkyl) hydrogen atoms are replaced by fluorine atoms. These carbon–fluorine bonds are among the strongest known single covalent bonds, contributing to the chemical and thermal stability of PFAS (Buck et al., 2011; Glenn et al., 2021; Wang et al., 2017). Their pervasive and potentially hazardous nature has led to their categorization as one of the most pressing environmental health concerns of the 21st century (Ng et al., 2021).

Since the 1940s, PFAS have been widely used in industrial and consumer products for their thermal stability, resistance to degradation, and hydrophobic and oleophobic properties (Cousins et al., 2019; Gaines, 2023; Malik et al., 2024). These substances, known as 'forever chemicals', resist natural degradation, making them difficult to detoxify or metabolize in biological systems (Manojkumar et al., 2023; Pelch et al., 2019). Consequently, these substances can accumulate and remain in the human body for approximately 3.8, 5.4 and 8.5 years for

* Corresponding author at: Department of Biology, University of Aveiro, 3810-193 Aveiro, Portugal.
E-mail address: rosafreitas@ua.pt (R. Freitas).

https://doi.org/10.1016/j.marpolbul.2025.118490
Received 7 June 2025; Received in revised form 19 July 2025; Accepted 22 July 2025
Available online 4 August 2025
0025-326X/© 2025 The Authors. Published by Elsevier Ltd. This is an open access article under the CC BY license (http://creativecommons.org/licenses/by/4.0/).

perfluorooctanoic acid (PFOA), perfluorooctane sulfonate (PFOS), and perfluorohexanesulfonic acid (PFHxS), respectively, which underscores their potential for long-term bioaccumulation and associated health risks even after exposure has ceased (Olsen et al., 2007). These properties have rendered them indispensable in different products, ranging from non-stick cookware to water-repellent textiles and firefighting foams (Podder et al., 2021). As a result, significantly high concentrations of PFAS have been found in different consumer items. Concentrations of perfluorohexanoic acid (PFHxA) ranging from < limit of detection (LOD) to 16,662 ng/g were found in smartwatch straps made from fluoroelastomers (Wicks et al., 2024). These results underscore concerns regarding dermal exposure, a pathway that has received comparatively less attention than ingestion or inhalation. In cosmetics, PFAS are employed due to their water-repellent and film-forming properties. Whitehead et al. (2021) detected fluorine in over 52 % of waterproof masks, 63 % of liquid lipsticks, and 47 % of foundations, with PFAS concentrations between 22 and 10,500 ng/g. Additionally, menstrual hygiene products, such as tampons and sanitary pads, have received comparatively minimal attention in terms of their potential as sources of PFAS exposure. A study by Good and Charbonnet (2024) found PFAS in all tested menstrual underwear, including nonmenstrual organic cotton, with concentrations up to 1.69 ng/g. The highest PFAS levels were in outer crotch layers, with inner gussets also containing PFAS, indicating potential exposure routes.

The widespread use of PFAS in industrial and consumer products has led to their extensive release into various environmental compartments, including water sources. According to Podder et al. (2021), PFAS concentrations in surface water systems have increased over the years worldwide (ng/L), with the predominance of perfluoroheptanoic acid (PFHpA) in Asia and China, while PFOA and PFOS are more prevalent in Europe and North America, respectively. In drinking water, PFAS have been detected across different countries worldwide (Heo et al., 2014; Li et al., 2021; Podder et al., 2021; Schwanz et al., 2016; Sörengård et al., 2022; Sun et al., 2016), with concentrations ranging from 1.6 ng/L of PFOS in France (Schwanz et al., 2016) to 324 ng/L of perfluorobutane sulfonic acid (PFBS) in Cape Fear River, North Carolina, United States (Sun et al., 2016). Estimated average daily intakes of PFOS and PFOA through drinking water consumption are approximately 0.17 to 0.21 ng/kg body weight per day, respectively (Gellrich et al., 2013). Also, in rivers, PFAS have been reported globally (An et al., 2023; Boiteux et al., 2017; Lorenzo et al., 2016; Möller et al., 2010; Pétré et al., 2022), with concentrations ranging from 2.5 ng/L - PFOA in the Jiulong River and Xiamen Bay, China (An et al., 2023) to 742.9 ng/L – perfluorobutanoic acid (PFBA) in the Guadalquivir River, Spain (Lorenzo et al., 2016). Being seawater the ultimate global destination for PFAS, compounds such as PFBA, PFOA, perfluorononanoic acid (PFNA), and PFOS are generally the most prevalent. Reported concentrations of total PFAS in seawater (Chen et al., 2016; Hung et al., 2020; Muir and Miaz, 2021; Wang et al., 2019; Zhang et al., 2019) ranged from 660 pg/L in the northwest Atlantic margin (Zhang et al., 2019) to 99.8 ng/L in the Bohai Sea, China (Chen et al., 2016). In estuarine environments, concentrations ranged from 39.9 ng/L in the Maribyrnong River, Australia (Ackerman Grunfeld et al., 2024), to 209 ng/L in the Shuangtaizi Estuary, China (Shao et al., 2016). The accumulation of PFAS in aquatic organisms is a growing concern due to their persistence, bioaccumulation, and potential impact on wildlife and human health *via* the food web. Studies have reported PFAS levels in bivalves and fish across various regions (Cunha et al., 2005; Fair et al., 2019; Giari et al., 2023; Young et al., 2022). For instance, the highest concentration reported was 126.4 ng/g PFOS in bleak (*Alburnus alburnus*), a sentinel species for quality control of rivers, from the river Po in Italy (Giari et al., 2023), while the lowest was 4 μg/kg, reported for the sum of 20 PFAS (Σ_{20}PFAS) in clams collected from the Washington, DC metropolitan area, which can be consumed by the human population, increasing the risk of bioaccumulation and toxicological effects (Young et al., 2022).

As PFAS are increasingly detected globally and in consumer products, regulatory frameworks are being introduced to address their widespread contamination, driven by growing awareness of their environmental persistence and potential health risks (Alazaiza et al., 2025). In the United States, the Environmental Protection Agency (USEPA) has introduced stringent measures under the Toxic Substances Control Act (TSCA) and the Safe Drinking Water Act (SDWA). The USEPA finalized the National Primary Drinking Water Regulation (NPDWR) in April 2024, which mandates a maximum contaminant level (MCL) in drinking water for PFOS and PFOA at 4 ng/L. Additionally, MCLs have been set for four other PFAS compounds: ammonium perfluoro(2-methyl-3-oxahexanoate) (GenX - 10 ng/L); perfluorobutanesulfonic acid (PFBS - 2 μg/L); PFNA - 10 ng/L; and PFHxS - 10 ng/L (USEPA, 2024). Before the implementation of the NPDWR, the USEPA had only regulated PFOS and PFOA, without establishing specific limits for other PFAS compounds or the total concentration of PFAS (USEPA, 2022). In contrast, the European Union (EU) has set a regulatory standard that mandates participating countries do not exceed a sum of 20 PFAS (Σ_{20}PFAS) concentration of 500 ng/L in drinking water. Each of the 20 individual PFAS [PFBA; PFPeA, PFHxA; PFHpA; PFOA; PFNA; PFDA; PFUnDA; PFDoDA; PFTriDA; PFBS; PFPeS; PFHxS; PFHpS; PFOS; PFNS; PFDS; PFUnDS; PFDoDS and PFTrDS] must not exceed 100 ng/L (European Commission, 2024). The European Chemicals Agency (ECHA) has proposed a comprehensive ban on all PFAS by 2025, further emphasizing its commitment to addressing these chemicals. Additionally, the EU also introduced environmental quality standards for PFOS at 0.65 ng/L and PFOA at 1.1 ng/L in surface waters to protect aquatic ecosystems (ECHA, 2024). Globally, Canada monitors and regulates PFAS emissions through the Environmental Protection Act, with a limit of 30 ng/L for the sum of 25 PFAS (Σ_{25}PFAS) and individual guidelines of 600 ng/L for PFOS and 200 ng/L for PFOA. Australia's National PFAS Position Statement sets action levels at 560 ng/L for PFOA and 70 ng/L for PFOS and GenX (Australia, 2024). Japan and Taiwan set drinking water limits for PFOS and PFOA at 50 ng/L, with Taiwan also establishing a 70 ng/L limit for GenX. As dietary intake is a primary PFAS exposure route, the European Food Safety Authority (EFSA) has updated its safety thresholds based on new scientific evidence. Initially, in 2008, EFSA established provisional tolerable daily intakes (TDIs) of 150 and 1500 ng·kg^{-1} bw·day^{-1} for PFOS and PFOA, respectively, based primarily on subchronic toxicity data from *Cynomolgus monkeys* (EFSA, 2008). However, as human epidemiological data availability increased, EFSA has re-evaluated these values. In 2018, new tolerable weekly intakes (TWIs) were proposed: 13 and 6 ng·kg^{-1} bw·week^{-1} for PFOS and PFOA, respectively (Knutsen et al., 2018). Subsequently, in 2020, EFSA further consolidated these limits, establishing a combined TWI of 4.4 ng·kg^{-1} bw·week^{-1} for the sum of PFOS, PFOA, PFNA, and PFHxS, reflecting updated risk assessments and a more conservative approach to long-term health protection (Schrenk et al., 2020; Sinclair et al., 2020). As a consequence of public awareness and increasing legislation, the phase-out of legacy PFAS, such as PFOS and PFOA, has driven the adoption of alternative short-chain compounds, often referred to as emerging PFAS (*e.g.*, GenX, PFBS, PFBA, PFHxS), which were designed to be less persistent in the environment (Ateia et al., 2019). However, research on these newer PFAS remains limited, and regulatory frameworks are still insufficient (Dean et al., 2020). Additionally, only a small proportion of the total PFAS released into the environment is routinely monitored (Dasu et al., 2022). Regulatory measures have led to a shift from long-chain to short-chain PFAS, which have fewer than seven carbon atoms. While short-chain PFAS are less bioaccumulative due to higher water solubility, their persistence in aquatic systems and potential for widespread dispersion raise concerns about long-term environmental and health impacts (Gewurtz et al., 2019; Mumtaz et al., 2019). For instance, PFBA has been used as a substitute for PFOA (Wang et al., 2024), and PFBS has replaced PFOS (Olsen et al., 2007, 2009) due to its shorter half-life in the environment. These compounds have been extensively detected in drinking water, sediments, sewage sludge, and even polar ice (Cai et al., 2012; Möller et al., 2010; Sun et al., 2016; Yan et al., 2012; Zhou et al., 2013).

In Xiaolangdi, China, short-chain PFAS accounted for up to 89 % of the total PFAS present in the aquatic environment, highlighting their prevalence (Zhao et al., 2016). Moreover, certain short-chain PFAS, like perfluorohexanoic acid (PFHxA) and PFHpA, may pose toxicological risks similar to PFOA (Apelberg et al., 2007; Du et al., 2015; Li et al., 2020). Their lower adsorption and high mobility in groundwater and soils lead to persistent environmental contamination. The ECHA proposed adding PFHxA to Article 57 of Regulation 1907/2006, highlighting its persistence despite mobility. While regulatory guidelines for short-chain PFAS are still developing, their widespread presence and concerning properties call for prompt action (Brendel et al., 2018).

Due to their widespread presence and potential risks, short-chain PFAS, though marketed as safer, may still pose environmental and toxicological threats, underscoring the need for deeper biological understanding. Therefore, this study aimed to compare the biochemical impacts induced by emerging (PFBA, PFBS, GenX, PFHxS) and classic (PFOA, PFOS, PFNA) PFAS, using S9 subcellular fractions (containing cytosolic enzymes) derived from the digestive gland and gills of mussels *Mytilus galloprovincialis*. Gills and digestive gland are commonly selected in biomonitoring studies with mussels, as they represent key target tissues for pollutant uptake and bioaccumulation, respectively, reflecting both immediate exposure and chronic effects. This research aims to compare the toxicological profiles of PFAS, assess their potential to disrupt enzymatic processes, and explore their environmental implications, contributing to the growing body of knowledge and informing regulatory strategies.

2. Materials and methods

2.1. Chemicals

The following PFAS compounds were acquired from SIGMA (Table 1): **Emerging** - heptafluorobutyric acid (PFBA, CAS number 375–22-4), nonafluorobutane-1-sulfonic acid (PFBS, CAS number 375–73-5), ammonium Perfluoro (2-methyl-3-oxahexanoate) (GenX, CAS number 62037–80-3) and perfluorohexanesulfonic acid (PFHxS, CAS number 355–46-4). These substances are classified as emerging due to their recent development and introduction as alternatives to traditional PFAS, primarily because of their shorter carbon chain lengths, which are assumed to reduce bioaccumulation and environmental persistence. **Legacy** - perfluorooctane sulfonic acid (PFOS, CAS number 1763-23-1), perfluorooctanoic acid (PFOA, CAS number 335–67-1), and perfluorononanoic acid (PFNA, CAS number 375–95-1). These compounds were widely used in the past but have been largely phased out due to their persistence in the environment and potential toxicological risks. However, they may still be of limited use and may still be present in legacy products and in the environment.

To prepare the primary stock solutions, each PFAS was dissolved in methanol, except for PFBA and PFBS, which were dissolved in distilled water. The stock solutions were made at a concentration of 200 mg/L and then diluted 10× with distilled water. Then, further serial dilutions were performed to obtain final concentrations of 1000, 100, 10, and 1 μg/L for use in the reaction mixtures, as described in section 2.2. The concentrations used in these tests (0.1; 1.0; 10.0 and 100.0 μg/L) were chosen considering several factors: European Union guidelines for drinking water quality (100–500 ng/L) as referenced by Dettori et al. (2022), environmental levels previously detected in monitoring studies (Bonato et al., 2020; Brusseau and Guo, 2022; Paige et al., 2024; Pétré et al., 2022; Sinclair et al., 2020; Zarębska et al., 2024), and concentrations demonstrated to impact marine invertebrates under controlled laboratory conditions (Bernardini et al., 2021; Copeto et al., 2024; Fabbri et al., 2014; Liu and Gin, 2018). A solvent control was included to ensure that the final methanol concentration did not affect the biological responses, confirming that biochemical changes were due solely to PFAS exposure. According to OECD guidelines, the methanol concentration in the test medium should be kept below 0.01 %. However, a single concentration of 0.05 % was tested, as it was required for preparing the 100 μg/L solution (OECD, 2019).

2.2. In vitro assays

Specimens of the mussel's species *Mytilus galloprovincialis* (shell length: 60.0 ± 3.0 mm; width: 33.0 ± 2.3 mm) were collected in the Ria de Aveiro coastal lagoon (Portugal) in September 2024. Afterwards, mussels were transported to the laboratory and maintained under controlled conditions (17 ± 1 °C and 30 ± 1 salinity) for two weeks to facilitate acclimation and depuration. During this period, mussels were fed daily with a mixture of three algae (*Phaeodactylum sp.*, *Tetraselmis sp.* and *Isochrysis galbana* 1:1:1). *M. galloprovincialis* was selected for this study due to its well-established role as a sentinel species in environmental monitoring. It has been extensively utilized in ecotoxicological research as a bioindicator of various classes of pollutants, including trace metals, organic contaminants, and emerging substances (Chahouri et al., 2023; Chiarelli and Roccheri, 2014; Kanduč et al., 2011;

Table 1
Overview of Per- and Polyfluoroalkyl Substances (PFAS) Tested and Corresponding Chemical Specifications. For each PFAS compound, the following information is shown: short name, Chemical Abstracts Service (CAS) number, molecular formula, number of fully fluorinated carbon atoms and chemical structure.

Compound	Short name	CAS	Molecular formula	Fluorinated carbons	Chemical structure
Heptafluorobutyric acid	PFBA	375–22-4	C_3F_7COOH	3	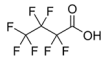
Nonafluorobutane-1-sulfonic acid	PFBS	375–73-5	$C_4F_9HF_9O_3SH$	4	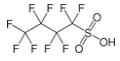
Ammonium Perfluoro(2-methyl-3-oxahexanoate)	GenX	62,037–80-3	$C_6H_4F_{11}NO_3$	5	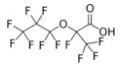
Perfluorohexanesulfonic acid	PFHxS	355–46-4	$C_6F_{13}SO_3H$	6	
Perfluorooctane sulfonic acid	PFOS	335–67-1	$C_8F_{17}SO_3H$	8	
Perfluorooctanoic acid	PFOA	376–06-7	$C_8HF_{15}O_2$	7	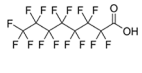
Perfluorononanoic acid	PFNA	375–95-1	$C_8F_{17}COOH$	8	

Tresnakova et al., 2023). After acclimation, mussels were dissected, and the digestive gland (DG) and gills (G) of 40 individuals were harvested, yielding eight tissue pools (four pools of 10 DG and four pools of 10 G). Subsequently, these pools were homogenized with phosphate buffer (K_2HPO_4, 0.1 M, pH 8.2) at a 1:2 (*w/v*) ratio using a Potter Elvehjem homogenizer. The homogenates were then centrifuged at 10,000 *g* for 20 min at 4 °C, and the resulting supernatants (S9 fractions, which contain cytosolic enzymes) were collected, aliquoted, and stored at −80 °C for further analysis. Before *in vitro* exposures, the protein (PROT) concentration was determined to prevent enzyme saturation and ensure precise enzyme kinetics. The S9 fractions were diluted to 1 mg/mL PROT (obtained by diluting the supernatants in 0.1 M K_2HPO_4, pH 8.2), following OECD No. 319B guidelines (OECD, 2018), except for tests assessing total antioxidant capacity (TAC) and lipid peroxidation (LPO) levels. For these parameters, the samples were not standardized to PROT concentration, as they reflect contents rather than enzyme activity. S9 fractions of DG and G tissues were isolated, and four replicates of each pool of tissue were exposed to four concentrations of each PFAS (0.1; 1.0; 10.0 and 100.0 μg/L) in addition to the control (CTL – without PFAS) and the solvent control (CTL methanol) for 30 min. After the 30 min exposure at 25 ± 1 °C on an orbital shaker (1200 rpm), biochemical measurements were performed as described in section 2.3 and in Table 2. The incubation conditions (PROT concentration, duration, and temperature) were chosen based on prior research (Giannessi et al., 2023; Vieira Sanches et al., 2023), which indicated that these conditions are effective for evaluating enzymatic activity in *in vitro* models. These

Table 2
The Biochemical parameters evaluated, the respective function, the methodology applied, spectrophotometric readings, extinction coefficient/standard, the expression units and the respective reference.

Biochemical Parameter	Function	Methodology applied	Spectrophotometric readings (nm)	Extinction coefficient (M^{-1} cm^{-1}) / Standard	Expression Units	Reference
PROT	Structural component / Energy reserve	The biuret assay was performed using bovine serum albumin (BSA) as the standard. In this technique, copper(II) ions in the Biuret reagent interact with peptide bonds in amino acids under alkaline conditions to form a coordination complex. This reaction results in a colour change from blue to purple, indicating the presence of proteins.	540	- / 0–40 mg/L	mg/g FW	Robinson and Hogden, 1940
SOD	Antioxidant enzyme	This assay is based on the ability of Cu—Zn SOD to inhibit pyrogallol autoxidation.Under alkaline conditions (pH 8.2) and in the presence of EDTA, approximately 50 % of pyrogallol undergoes autoxidation.The extent of inhibition by SOD serves as a quantitative indicator of enzymatic activity, reflecting its role in superoxide radical dismutation.	560	–	U/mg PROT, U represents a inhibition of 50 % of pyrogallol autoxidation	Magnani et al., 2000
CAT	Antioxidant enzyme	The CAT activity assay is based on the enzyme's ability to catalyze the decomposition of H_2O_2 into H_2O and O_2. After the addition of 30 mM H_2O_2, the reaction is monitored spectrophotometrically by measuring the decrease in absorbance during 2 min. The rate of absorbance reduction directly correlates with the activity of CAT.	240	43.5 / -	U/mg PROT, U represents the μmol of H2O2 consumed per min	Aebi, 1984
TAC	Antioxidant content	The TAC levels is a method of measuring the antioxidant capacity by assessing its ability to reduce ferric ions (Fe^{3+}) to ferrous ions (Fe^{2+}). This reduction process leads to the formation of a blue-coloured complex, known as the ferrous-tripyridyltriazine, which can be measured quantitatively using spectrophotometry.	593	0–1000 μM / -	μmol/g FW	Benzie and Strain, 1996 and adapted by Hagger et al., 2005
CbEs	Phase I biotransformation	*P*-nitrophenyl butyrate (pNPB) was utilized as the substrate for this reaction. The hydrolysis rate of pNPB was measured over a 5 min period in order to ascertain CbEs enzyme activity.	405	18,000	nmol/min/mg PROT	Hosokawa and Satoh, 2001 and adapted by Solé et al., 2018
GSTs	Phase II biotransformation	In this protocol, GSTs catalyze the conjugation of 1-chloro-2,4-dinitrobenzene (CDNB) with the thiol group of reduced glutathione (GSH), resulting in the formation of a thioether. The increase in absorbance is monitored for 5 min, with the rate of absorbance change directly proportional to the GSTs activity.	340	9600	nmol/min/mg PROT	Habig et al., 1974 adapted by Carregosa et al., 2014
LPO	Cellular damage	Thiobarbituric acid reactive substances (TBARS), formed through the interaction of LPO by-products, specifically malondialdehyde (MDA), with 2-thiobarbituric acid (TBA), were utilized to spectrophotometrically assess the levels of LPO.	532	156,000	nmol MDA/g FW	Ohkawa et al., 1979
AChE	Neurotransmission	Acetylthiocholine iodide (ATChI) was utilized as the substrate in the enzymatic reaction, resulting in the production of thiocoline. Upon the addition of Ellman's reagent (DTNB), the dianion of 5-thio-2-nitrobenzoic acid (TNB) is generated.	412	13,600	nmol/min/mg PROT	Ellman et al., 1961 and adapted by Mennillo et al., 2017

studies identified that a 30 min exposure at 25 °C with 1 mg of PROT resulted in the highest enzyme activity and substrate transformation rates. Moreover, these studies showed no significant differences in the analyzed parameters when comparing exposure times of 30 and 60 min.

2.3. Biochemical parameters

To evaluate the biochemical alterations triggered in mussels' organs following exposure to seven PFAS (PFBA, PFBS, GenX, PFHxS, PFOS, PFOA and PFNA), a set of biochemical parameters was employed as biomarkers (Table 2). These parameters encompassed: i) antioxidant enzyme activities, specifically superoxide dismutase (SOD) and catalase (CAT) activities and total antioxidant capacity (TAC); ii) biotransformation enzyme activities, such as carboxylesterases (CbEs) and glutathione S-transferases (GSTs); iii) cellular damage, measuring levels of lipid peroxidation (LPO) and iv) neurotransmission, by measuring the activity of the enzyme acetylcholinesterase (AChE). The quantification of PROT content to a standardized working protein concentration of 1 mg/mL for *in vitro* assays was carried out (results expressed in mg/mL).

2.4. Data analysis

2.4.1. Statistical analyses

The statistical analysis of biochemical parameters (SOD, CAT, TAC, CbEs, GSTs, LPO and AChE) for all replicates ($n = 4$, 10 mussels per replicate, tissue, and PFAS concentration) was performed using a non-parametric permutational multivariate analysis of variance (PERMANOVA). This analysis was conducted with the PRIMER v7 software, incorporating the PERMANOVA extension (Anderson et al., 2008). Initially, the data were square root transformed, followed by the creation of a resemblance matrix based on euclidean distances, chosen to accommodate the different units in the biochemical measurements. The matrix was analyzed using type III sums of squares with unrestricted permutation of the raw data across 9999 permutations. A *p*-value of <0.05 was considered statistically significant and the following three null hypotheses were tested for each organ: *i*) no significant differences among different concentrations of each PFAS in each organ (if rejected, significant differences are highlighted with lower case letters in figures); *ii*) no significant differences compared to control condition (if rejected, significant differences are highlighted with an asterisk in figures); *iii*) no significant differences among PFAS for each concentration (if rejected, significant differences are highlighted by bold *p*-values in supplementary material (SM) Tables 1 and 2.

2.4.2. Integrated biological response (IBR) index

The Integrated Biomarker Response index, version 2 (IBR v2), was employed to integrate the data from all measured biochemical parameters and to illustrate the overall biochemical response patterns in S9 fractions of *M. galloprovincialis* DG and G subjected to different PFAS (PFBA; PFBS; GenX; PFHxS; PFOS; PFOA; PFNA) at different concentrations (0.1; 1; 10; 100 μg/L). This approach, originally developed by Beliaeff and Burgeot (2002) and later adapted by Sanchez et al. (2013), was used to compare biochemical variations between mussels' organs exposed to different concentrations of PFAS, relative to the control (CTL) group (0 μg/L). To normalize the data and reduce variability, a logarithmic transformation (Y_i) was applied using the formula $Y_i = \log(X_i / X_0)$, where X_i represents the biomarker value for a given treatment, and X_0 denotes the average value from the CTL group. The transformed data were then standardized using $Z_i = (Y_i - \mu) / \sigma$, with μ and σ corresponding to the overall mean and standard deviation of Y_i, respectively. A deviation index ($A = Z_i - Z_0$) was calculated to center the data around zero, thereby emphasizing deviations relative to the CTL condition. The final IBR score was obtained by summing the absolute values of A (IBR v2 $= \Sigma|A|$), with results visually presented in Figs. 5 and 6, where the bar graph was used to show the final IBR score for all treatments and the radar plots illustrate the contribution of each biomarker to the overall IBR score.

2.4.3. Non-metric multidimensional scaling (nMDS)

The biochemical data for each concentration for each PFAS was used to calculate the average for each PFAS and then analyzed using ordination techniques, specifically Non-metric Multidimensional Scaling (nMDS), carried out using PRIMER v7 software. A distance matrix was created using Euclidean distance, which was then normalized for the analysis. The resulting two-dimensional plot (with horizontal and vertical axes) included a stress value that reflects the accuracy of the multidimensional representation (Clarke et al., 2001). A stress value below 0.10 indicates a very good fit, while values above 0.30 suggest that the plot does not accurately represent the distance matrix (Clarke et al., 2001). Vectors from biochemical data were included in the nMDS analysis by Pearson correlation that had a correlation value exceeding 0.25.

3. Results

3.1. Biochemical parameters

3.1.1. Antioxidant defenses

In digestive gland (DG), for each PFAS, significant differences in SOD activity among concentrations were found for all PFAS except for PFHxS and PFOA. At 1 μg/L, PFBA and GenX showed significantly lower activity compared to the remaining concentrations, while PFBS, PFOS, and PFNA showed significantly reduced activity at 10 and 100 μg/L, compared to the remaining concentrations. In gills (G), among concentrations in each PFAS, at 1 μg/L of PFBS and GenX, at 10 and 100 μg/L of PFBA and PFNA and at 100 μg/L of PFOS there was a significantly lower activity compared to other concentrations (Fig. 1A). Compared to CTL in DG, PFBS at 0.1 and 1 μg/L induced significantly higher SOD activity, while PFBA (0.1 μg/L), GenX (1 μg/L), PFOS (100 μg/L), PFNA (10 and 100 μg/L), PFHxS and PFOA at all concentrations showed significantly lower activity (Fig. 1A). In G, SOD activity was significantly lower than CTL across all concentrations of PFHxS, PFOS, PFOA, and PFNA, whereas PFBA induced a significant increase regardless of the concentration tested (Fig. 1A). In DG, at each concentration, comparisons between PFAS, showed a significant increase in SOD activity for PFBS, compared to the other PFAS (Table 1SM). For G, SOD activity was significantly higher in PFBA and GenX across all concentrations, especially in comparisons against PFHxS, PFOS, and PFOA (Table 2SM).

Regarding CAT activity in DG, significantly lower and higher activities compared to other concentrations were observed at 100 μg/L for GenX and 10 μg/L for PFBS, respectively. In G, PFBS showed significantly higher CAT activity at 10 μg/L, whereas significantly lower activity was detected for PFHxS (10 μg/L) and PFOS (1, 10, 100 μg/L) (Fig. 1B). Compared to CTL, for each PFAS and concentration, significantly higher activity was found in DG only at 10 μg/L for PFNA and in G at 100 μg/L for GenX (Fig. 1B). Comparisons between PFAS for each concentration in DG, at 10 and 100 μg/L, significantly higher activity was detected for PFNA in comparison with PFBA and GenX (Table 1SM). In G, in general, significantly higher activity of CAT was observed at higher concentrations (10 and 100 μg/L), particularly in PFBS and GenX, compared to PFHxS and PFOS (Table 2SM).

The levels of TAC, in DG, showed a significant decrease for PFOA at concentrations of 10 and 100 μg/L, while no significant differences were observed for other PFAS across concentrations. In G, no significant differences were found among concentrations, regardless of the PFAS (Fig. 1C). Compared with the CTL values in DG, PFBA, PFBS, and GenX showed significantly lower levels regardless of the concentration, while in the G, no significant differences were found compared to the CTL (Fig. 1C). Comparing PFAS at different concentrations, TAC levels were significantly lower in PFBA, especially at lower concentrations, when compared to PFOS, PFOA and PFNA. Moreover, in DG, at the higher concentrations (100 μg/L), PFOA demonstrated a significant decrease in

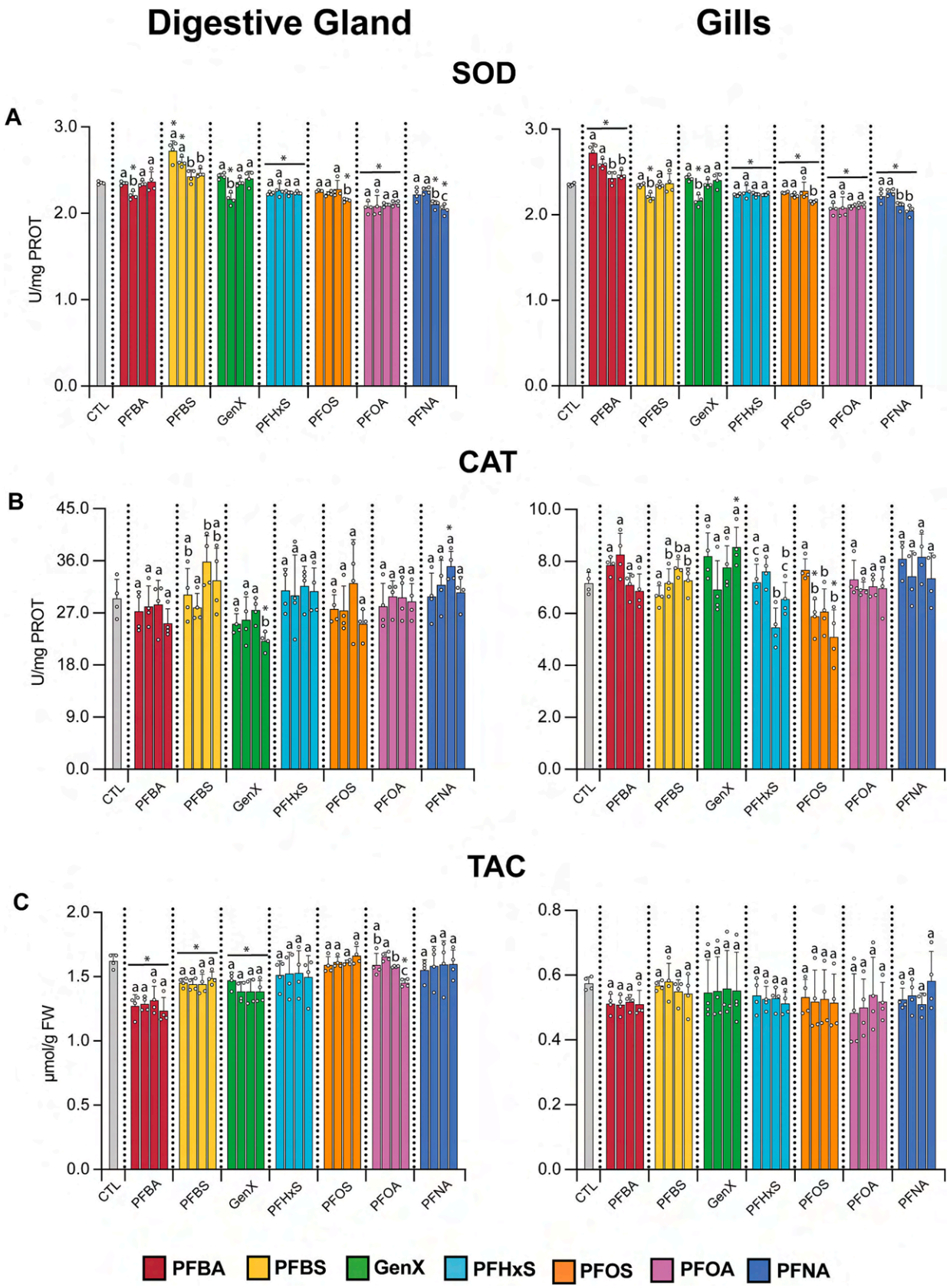

Fig. 1. **A:** Superoxide Dismutase (SOD) activity; **B:** Catalase (CAT) activity; **C:** Total Antioxidant Capacity (TAC) of S9 *Mytilus galloprovincialis* digestive gland and gills exposed to different treatments (CTL; PFBA; PFBS; GenX; PFHxS; PFOS; PFOA and PFNA) at different concentrations (0.1; 1.0; 10 and 100 ng/L). Results are reported as mean + SD. Significant differences ($p < 0.05$) among different concentrations of the same PFAS are indicated by different letters and compared to the CTL by an asterisk (*). $N = 4$, corresponding to 10 mussels *per* pool *per* tissue.

TAC in comparison with PFOS and PFNA (Table 1SM). In G, there were no significant differences in TAC across all treatments and concentrations (Table 2SM).

3.1.2. Detoxification enzyme activities

In DG, the activity of CbEs showed no significant differences among concentrations, regardless of the PFAS. In G, PFBS showed significantly higher activity at 100 μg/L compared to 1 and 10 μg/L (Fig. 2A). In DG, compared to the CTL, no significant differences were found regardless of the PFAS and concentration tested, while in G, significantly lower activity was detected for PFBA and PFHxS concentrations, and higher activity for GenX concentrations (Fig. 2A). Comparing different PFAS at each concentration, in the DG, CbEs activity showed a significant inhibition of PFHxS and PFOA at the higher concentration compared to PFNA (Table 1SM). In G, significantly lower activity in PFBA and PFHxS was observed at the lower concentrations (0.1 and 1 μg/L) compared to the remaining PFAS, and a significantly higher activity in GenX across all PFAS at each concentration (Table 2SM).

In relation to the activity of GSTs, no significant differences were observed among concentrations, regardless of the organ and the PFAS (Fig. 2B). In DG, compared to CTL with each PFAS concentration, PFHxS at 0.1 and 100 μg/L and PFNA at 0.1, 1, 100 μg/L showed significantly lower activity, and the same trend was detected in G for PFOS at 1, 10 and 100 μg/L and PFNA at 1 μg/L (Fig. 2B). Comparing the concentrations of different PFAS in DG, PFBS exhibited significantly higher activity compared to PFHxS, PFOA and PFNA (Table 1SM). The results demonstrated that G exhibited significantly higher GSTs activity in the presence of PFBA in comparison to PFOS and PFNA, regardless of the concentration (Table 2SM).

3.1.3. Cellular damage

In DG and G, there were no significant differences in the LPO levels among concentrations regardless of the PFAS (Fig. 3). For each PFAS, comparing each concentration with CTL, no significant differences were observed in DG. Conversely, in G, PFOA showed significantly lower levels regardless of the concentration (Fig. 3). Comparisons between PFAS at each concentration, in DG, the LPO levels showed significantly higher levels in PFOS in comparison with GenX, PFHxS and PFOA (Table 1SM). In G, all tested concentrations of PFOA exhibited significantly lower LPO levels in comparison with the remaining PFAS. Furthermore, mussels exposed to GenX showed significantly higher LPO levels than mussels exposed to PFBA and PFHxS, regardless of the concentration tested (Table 2SM).

3.1.4. Neurotransmission

The activity of AChE, in DG, for each PFAS among concentrations was significantly higher for GenX, PFOS and PFNA at 10 μg/L, PFHxS at 10 and 100 μg/L and for PFOA at 100 μg/L, while in PFBS at 1 μg/L the activity was significantly lower. In G, for each PFAS among concentrations, PFBA at 100 μg/L, PFHxS at 1, 10 and 100 μg/L and PFNA at 10 and 100 μg/L showed significantly lower activity (Fig. 4). For each PFAS, comparing all concentrations compared with CTL, in the DG, the activity of AChE was significantly lower in PFBS at 1 μg/L and PFOS at 0.1 and 1 μg/L and significantly higher in PFBA, GenX at 10 μg/L, PFOS

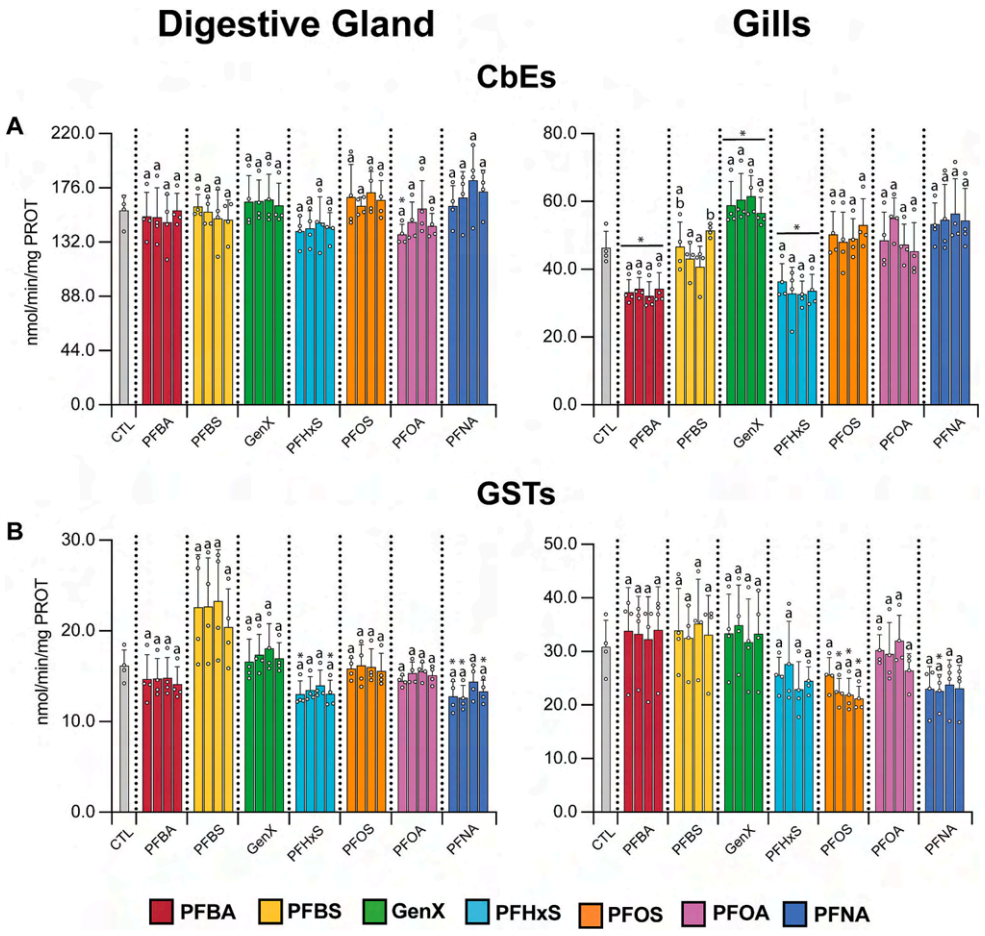

Fig. 2. **A:** Carboxylesterase (CbEs) activity; **B:** Glutathione S-transferases (GSTs) activity of S9 *Mytilus galloprovincialis* digestive gland and gills exposed to different treatments (CTL; PFBA; PFBS; GenX; PFHxS; PFOS; PFOA and PFNA) at different concentrations (0.1; 1.0; 10 and 100 ng/L). Results are reported as mean + SD. Significant differences ($p < 0.05$) among different concentrations of the same PFAS are indicated by different letters and compared to the CTL by an asterisk (*). N = 4, corresponding to 10 mussels *per* pool *per* tissue.

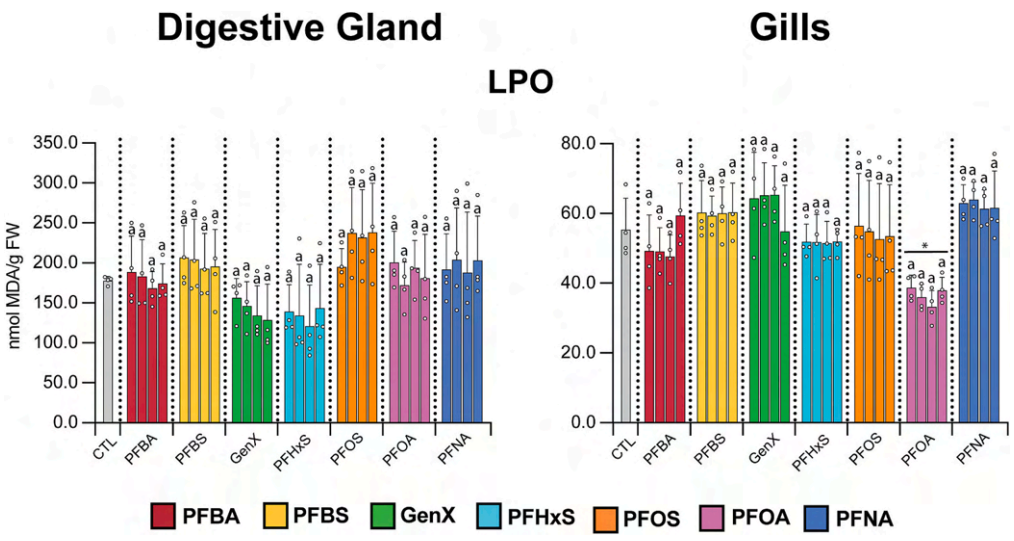

Fig. 3. Lipid peroxidation (LPO) levels of S9 *Mytilus galloprovincialis* digestive gland and gills exposed to different treatments (CTL; PFBA; PFBS; GenX; PFHxS; PFOS; PFOA and PFNA) at different concentrations (0.1; 1.0; 10 and 100 ng/L). Results are reported as mean + SD. Significant differences ($p < 0.05$) among different concentrations of the same PFAS are indicated by different letters and compared to the CTL by an asterisk (*). N = 4, corresponding to 10 mussels *per* pool *per* tissue.

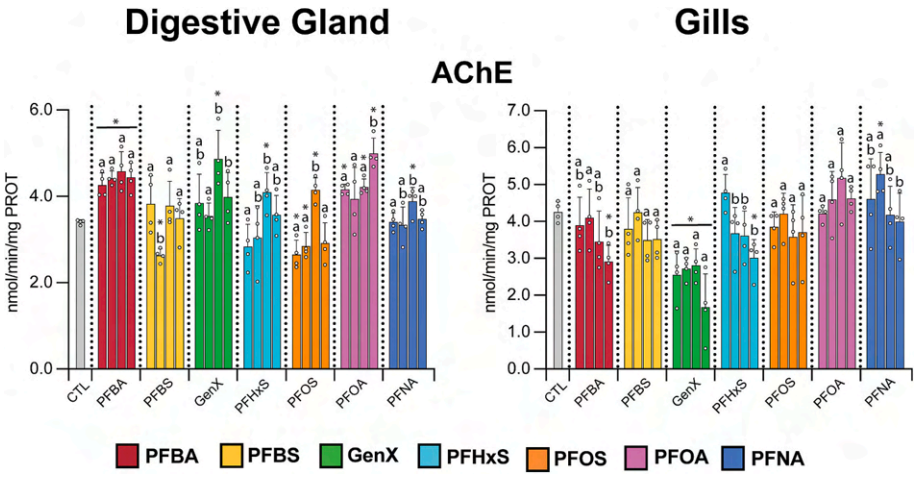

Fig. 4. Acetylcholinesterase (AChE) activity of S9 *Mytilus galloprovincialis* digestive gland and gills exposed to different treatments (CTL; PFBA; PFBS; GenX; PFHxS; PFOS; PFOA and PFNA) at different concentrations (0.1; 1.0; 10 and 100 ng/L). Results are reported as mean + SD. Significant differences ($p < 0.05$) among different concentrations of the same PFAS are indicated by different letters and compared to the CTL by an asterisk (*). N = 4, corresponding to 10 mussels *per* pool *per* tissue.

at 10 μg/L, PFOA at 0.1, 1 and 10 μg/L and PFNA at 10 μg/L. In G, significantly lower activity was found in PFBA at 1 μg/L, GenX at all concentrations, PFHxS at 100 μg/L, while significantly higher activity was found in PFNA at 1 μg/L (Fig. 4). In DG, comparing different PFAS for each concentration, PFHxS and PFOS at lower concentrations (0.1 and 1 μg/L) showed significant inhibition in comparison with PFBA and PFOA. At the highest concentration, PFOA exhibited a significant increase in AChE activity in comparison to the remaining PFAS (Table 1SM). In G, AChE activity was significantly lower across concentrations between PFAS, with GenX and PFBA frequently differing from PFOS, PFHxS, PFOA, and PFNA, especially at 10 and 100 μg/L (Table 2SM).

3.1.5. Solvent control

Among the biochemical parameters, 0.05 % methanol exhibited no significant differences in the DG and G compared to the CTL (Table 3SM).

3.2. Multivariate analysis

3.2.1. Integrated biomarker response (IBR) index

According to the IBR v2, DG exposed to emerging PFAS – PFBA, PFBS, GenX and PFHxS - achieved the highest values corresponding to 5.9, 4.5, 5.4 and 4.8, respectively. This indicates a more pronounced effect of DG in the presence of emerging PFAS compared to legacy, PFOS, PFOA and PFNA, which achieved lower IBR v2 values corresponding to 3.5, 4.2 and 4.3, respectively (Fig. 6). From the radar plot, higher IBR values in emerging PFAS were due to the increase of the activities of AChE, SOD (especially PFBA), CAT (especially PFBS and PFHxS), GSTs (especially PFBS), and a decrease of TAC and LPO (especially for GenX and PFHxS) levels. For legacy PFAS, the score was due to an increase in AChE activity in the presence of PFOS and PFOA, an increase in CAT and CbEs activities in PFOS and PFNA, and an increase in LPO levels in PFOS (Fig. 5). In G, IBR v2 values were similar among PFAS (IBR v2 between 4.9 and 5.5), except for PFBS, which

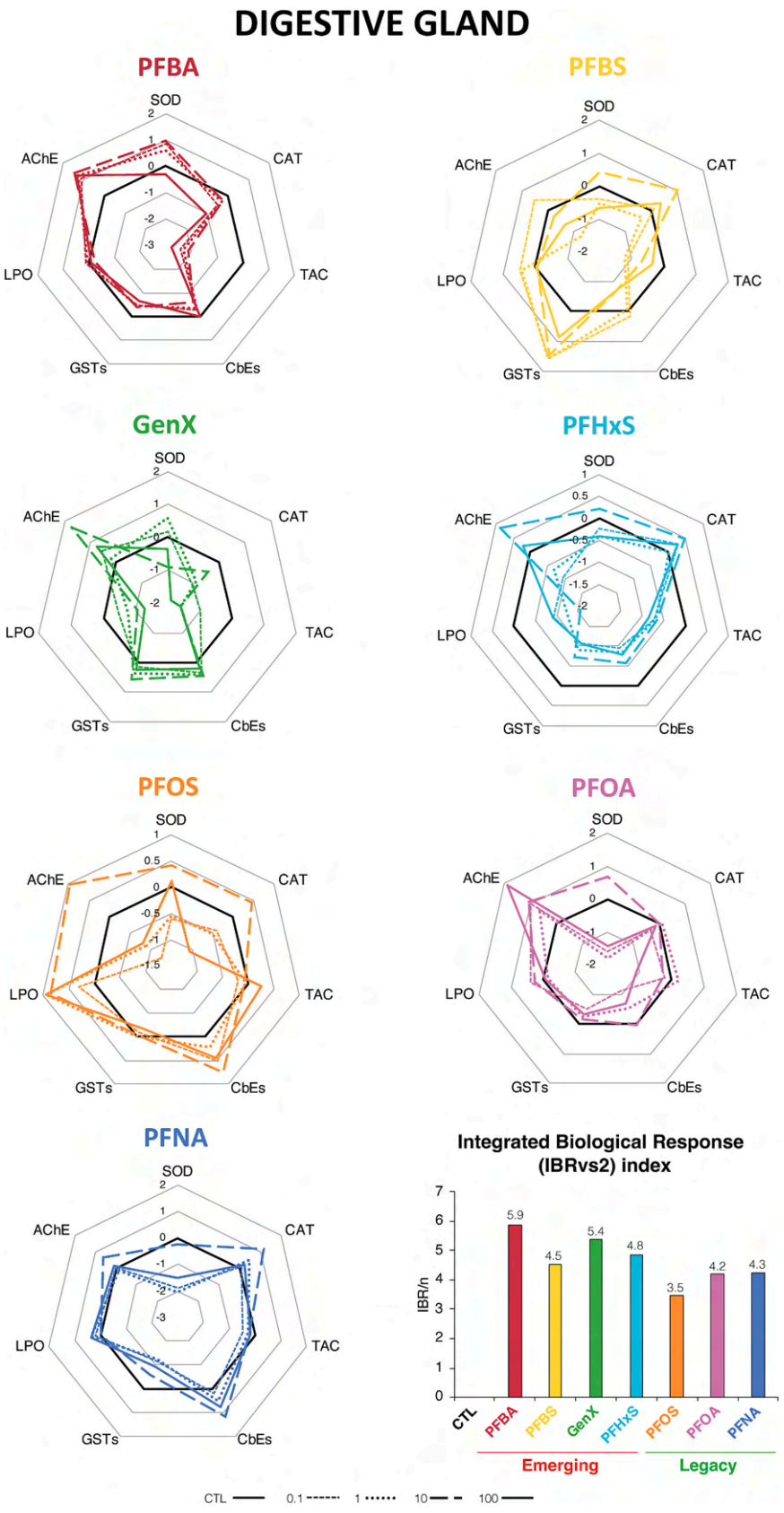

Fig. 5. Integrated Biomarker Response (IBR v2) index for each PFAS in comparison to control considering all biochemical parameters used on S9 *Mytilus galloprovincialis* digestive gland after *in vitro* exposure to different concentrations (0.1; 1; 10; 100 μg/L). The biomarker quantified for uncontaminanted digestive gland (control treatment) was considered for the reference line. SOD = Superoxide dismutase activity; CAT = Catalase activity; TAC = Total Antioxidant Capacity; CbEs = Carboxylesterases activity; GSTs = Glutathione S-transferases activity; LPO = Lipid peroxidation levels and AChE = Acetylcholinesterase activity. The black dashed line corresponds to control while the different dashed patterns relate to each concentration in each IBR related PFAS.

showed the lowest value (IBR v2 = 1.8). The radar plot revealed that PFBS exhibited a pronounced inhibition of AChE activity, a trend that was also observed for PFBA and GenX. However, an increase in activity was only noted in PFHxS at a concentration of 0.1 μg/L. Furthermore, PFBA demonstrated an increase in SOD activity, a decrease in TAC levels and CbEs activity, a similar effect to that observed for PFHxS, while GenX showed an induction of CbEs activity (Fig. 7). Concerning legacy PFAS, the graphical representation obtained demonstrated a similar pattern between PFOS, PFOA and PFNA. This pattern included an increase in CbEs activity, an increase in AChE activity, especially in PFOA and PFNA, an inhibition of GSTs activity, especially in PFOS and PFNA, and an increase and decrease in LPO levels, respectively, in PFNA and PFOA (Fig. 6).

3.2.2. Non-metric multidimensional scaling (nMDS)

The nMDS provided a two-dimensional ordination of experimental results, highlighting 2 main clusters, one with emerging and ther with legacy PFAS. In DG, a more pronounced dispersion was detected for emerging PFAS compared to the G, with PFHxS and PFBS furthest apart and PFBA and GenX closest together, thus showing a greater variability of responses than in the G. In contrast, this pattern was not observed in the G, where the emerging PFAS exhibited a more clustered distribution, suggesting lower variability in their effects. Conversely, legacy PFAS displayed a smaller difference in dispersion between the DG and G, indicating a more consistent mode of action across both organs (Figs. 7A and B).

The nMDS results for the DG showed that CTL, PFOS, PFNA, PFHxS, PFBS, and PFOA, GenX, PFBA, are on the positive and negative, respectively, side of the nMDS1 axis. In the axis of the nMDS2, GenX, PFBS, PFOS, PFNA, and PFBA, PFOA, PFHxS, and CTL are located on the positive and negative sides, respectively (Fig. 7A). A positive correlation with the negative axis of nMDS1 was associated with the SOD and AChE activities and PFBA and GenX. Conversely, PFBS and GSTs activity exhibited a positive correlation along the positive axis of the nMDS2, while PFHxS and this enzyme demonstrated a positive correlation along the negative axis of the nMDS2. Furthermore, it is evident that PFNA (a legacy PFAS), as well as TAC and CAT activity, demonstrated a positive correlation placed in the positive axis of nMDS1. In contrast, PFOS, CbEs activity and LPO levels showed a positive correlation that was placed on the positive axis of nMDS2 (Fig. 7A).

Regarding G, PFBA, PFBS, CTL, GenX, and PFHxS, PFOA, PFOS, and PFNA are on the positive and negative, respectively, sides of the nMDS1 axis. In respect of nMDS2, PFOS, PFOA, PFHxS, PFBA, GenX, and PFBS, PFNA, CTL are on the positive and negative sides, respectively, of the axis (Fig. 7B). The activity of SOD and PC levels exhibited a positive correlation, situated on the positive axis of nMDS2 with PFBA. Conversely, GSTs activity and GenX demonstrated a positive correlation, positioned on the positive axis of nMDS1. The activity of CAT and CbEs showed a positive correlation on the positive axis of nMDS1 with PFBS, while LPO and TAC levels showed a positive correlation with CTL on the negative axis of nMDS2. The legacy PFAS (PFOA, PFOS and PFNA) and AChE activity demonstrated a strong correlation, situated on the negative axis of nMDS1 (Fig. 7B).

4. Discussion

This study addressed critical knowledge gaps by employing *in vitro* assays to compare the biochemical interactions of legacy and emerging PFAS in the digestive gland (DG) and gills (G) of *Mytilus galloprovincialis*, a sentinel species widely used in environmental toxicology. The findings provide novel evidence of the capacity of both PFAS groups to disrupt key mechanisms involved in oxidative stress response, detoxification, and cellular homeostasis. These insights enhance the current understanding of PFAS toxicity and highlight the relevance of tissue-specific analyses in evaluating the environmental risks posed by structurally diverse PFAS compounds.

4.1. Legacy and emerging PFAS: Toxicological profiles

The present study revealed significant differences in the toxicological effects of legacy (PFOS, PFOA, PFNA) and emerging (GenX, PFBA, PFBS, PFHxS) PFAS in both tissue types under study. Multivariate analysis results revealed two distinct groups of PFAS: one including the emerging compounds (GenX, PFBA, PFBS, PFHxS) and another one, the legacy compounds (PFOS, PFOA, PFNA). This grouping is particularly evident for DG, where the IBR v2 index indicates markedly higher biological disturbance for several emerging compounds, particularly PFAS. The multivariate analysis further revealed a greater dispersion of emerging PFAS compared to legacy compounds in DG. This pattern suggests that emerging PFAS elicit more variable and pronounced biochemical responses in this tissue. Conversely, such differentiation between PFAS types is less pronounced in the G. In this organ, the IBR v2 values demonstrate greater homogeneity across both emerging and legacy compounds, suggesting a more uniform biological impact. Similarly, the multivariate analysis conducted with the G responses demonstrated a reduced degree of dispersion among PFAS treatments, thereby indicating that both groups elicit more analogous biochemical response profiles in this organ. This discrepancy between tissues may be attributed to differences in physiological roles, exposure pathways, or metabolic capacities. The DG, as a central organ responsible for the processes of detoxification and metabolism, may exhibit greater specificity and sensitivity to the chemical nature of PFAS, resulting in a more diverse range of responses. Conversely, the G, being in direct contact with the external aquatic environment, may respond more uniformly regardless of PFAS class, possibly due to consistent exposure dynamics or limited metabolic differentiation among compounds. Comparable patterns were reported by Pereira et al. (2025) and Giannessi et al. (2023), where *in vitro* exposures of S9 subcellular fractions of *M. galloprovincialis* G and DG to pharmaceutical compounds (gentamicin/diclofenac and veterinary fluoroquinolones, respectively) demonstrated that the DG exhibited a broader and more heterogeneous response profile across different contaminants and concentrations, as evidenced by principal coordinate ordination (PCO) analyses.

4.2. Tissue-specific biochemical responses to emerging and legacy PFAS

In this study, the discussion of PFAS-induced biochemical effects is structured according to the functional relevance and susceptibility of the analyzed tissues. The DG is addressed first, as it plays a central role in metabolism and detoxification processes and is often recognized as a primary and legacy target of environmental contaminants. Subsequently, the focus shifts to the G, a key interface tissue involved in gas exchange and directly exposed to the surrounding aquatic environment. This sequential approach allows for a clearer understanding of the tissue-specific nature of PFAS toxicity and facilitates a comparative interpretation of the observed biochemical responses.

4.2.1. Digestive gland

In the DG, the present study has demonstrated that exposure to emerging PFAS was associated with an increase in acetylcholinesterase (AChE) activity. This general upregulation suggests that these substances may interfere with cholinergic signaling pathways beyond the nervous system, potentially impacting physiological processes within the digestive tissues. Although AChE is traditionally recognized for its role in terminating synaptic transmission by hydrolyzing acetylcholine in neuronal tissues, its presence and regulation in non-neuronal sites, such as DG, are increasingly understood to be involved in modulating cell proliferation, differentiation, and immune or digestive functions (Faggio et al., 2018). Among the emerging PFAS tested, PFBA, GenX, and PFHxS induced particularly marked elevations in AChE activity, implying a strong perturbation of cholinergic-like mechanisms or cellular signaling pathways within the tissue. This response may be indicative of a compensatory or adaptive mechanism triggered by PFAS-

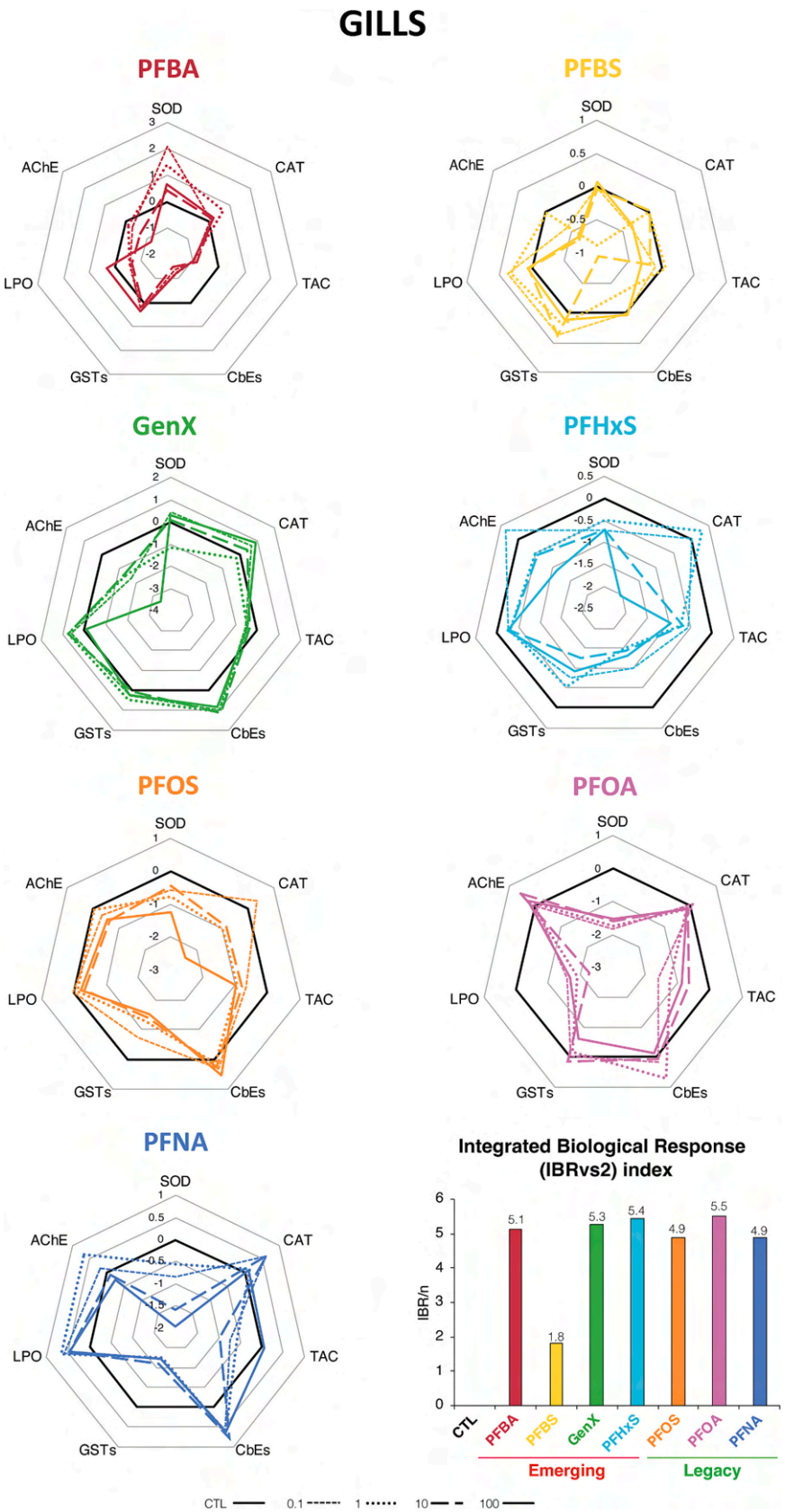

Fig. 6. Integrated Biomarker Response (IBR v2) index for each PFAS in comparison to control considering all biochemical parameters used on S9 *Mytilus galloprovincialis* gills after *in vitro* exposure to different concentrations (0.1; 1; 10; 100 μg/L). The biomarker quantified for uncontaminated gills (control treatment) was considered for the reference line. SOD = Superoxide dismutase activity; CAT = Catalase activity; TAC = Total Antioxidant Capacity; CbEs = Carboxilesterases activity; GSTs = Glutathione S-transferases activity; LPO = Lipid peroxidation levels and AChE = Acetylcholinesterase activity. The black dashed line corresponds to control while the different dashed patterns relate to each concentration in each IBR related PFAS.

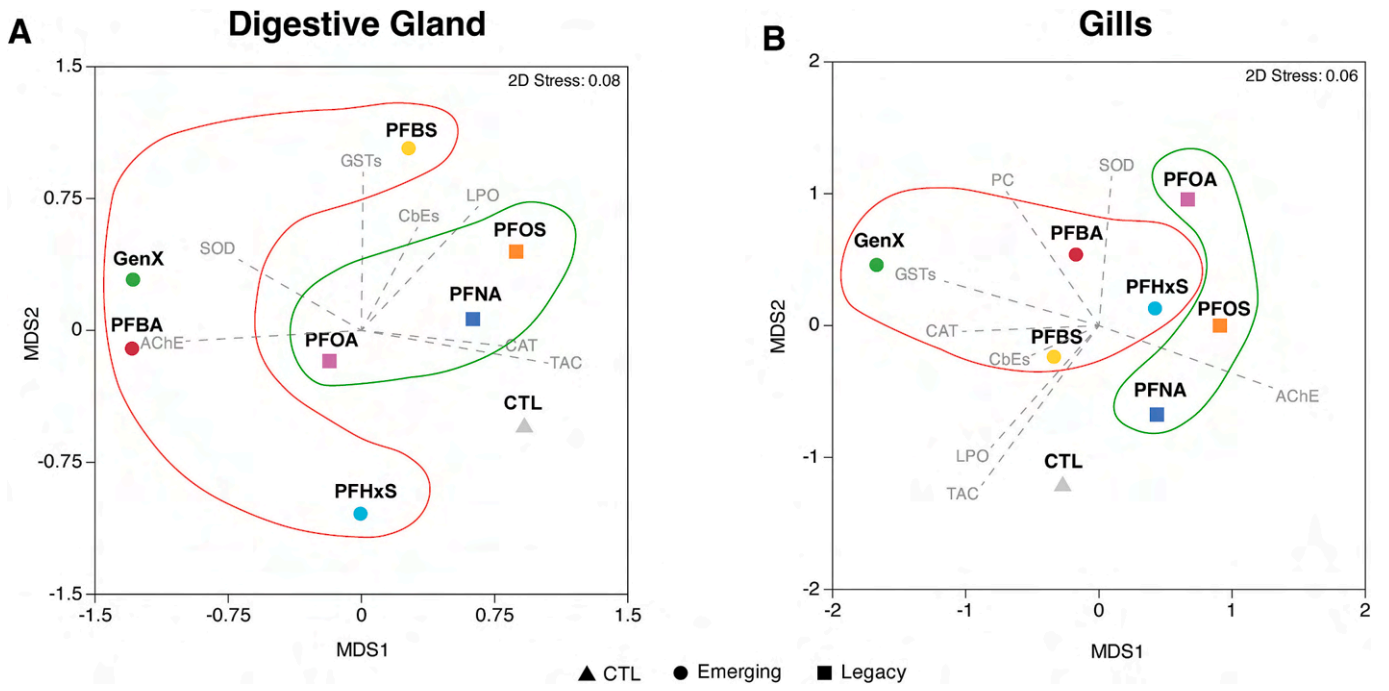

Fig. 7. Non-metric multidimensional scaling (nMDS) based on biochemical markers in S9 *Mytilus galloprovincialis* digestive gland (A) and gills (B) exposed to different concentrations (0.1; 1; 10; 100 μg/L). For nMDS, pearson correlation vectors are superimposed as supplementary variables, namely biochemical data ($r > 0.25$). SOD = Superoxide dismutase activity; CAT = Catalase activity; TAC = Total Antioxidant Capacity; CbEs = Carboxylesterases activity; GSTs = Glutathione S-transferases activity; LPO = Lipid peroxidation levels and AChE = Acetylcholinesterase activity.

induced cellular stress, particularly oxidative stress, which is known to influence the expression of various enzymes, including AChE. Furthermore, the upregulation of AChE in the DG may indicate a disruption in the homeostasis of acetylcholine, which plays an important role in non-neuronal cell signaling and can influence inflammatory and metabolic pathways. It is hypothesized that the increased AChE activity in the DG may affect the regulation of digestive enzyme production, secretory processes, and immune responses. This dysregulation has the potential to compromise digestive efficiency and immune competence, thereby reducing the organism's overall fitness and resilience to environmental stressors. Cruz et al. (2023) reported an increase in AChE activity in the DG of *M. galloprovincialis* following pharmaceutical exposures. The findings of the present study align with the results obtained, as the authors associated this effect with a short-term compensatory response aimed at counteracting the neurotoxic effects of the contaminants. However, it was also emphasized that AChE responses may vary depending on the specific contaminant and the duration of exposure. This is supported by the study conducted by Vieira Sanches et al. (2023), in which an *in vitro* exposure of mussel DG tissues to ionic liquids revealed that the activity of AChE was inhibited. These findings reinforce previous evidence that AChE activity is influenced by the specific chemical structure of the contaminant.

In terms of oxidative stress, the present study showed that the total antioxidant capacity (TAC), which reflects the overall ability of non-enzymatic cellular antioxidants, such as glutathione, vitamins C and E, and other small molecules, to neutralize reactive oxygen species (ROS), was inhibited in the DG following exposure to emerging PFAS, including GenX, PFBA, and PFHxS. This reduction is indicative of a diminished capacity to maintain redox homeostasis, thus suggesting a convergent oxidative stress response as a key toxicological mechanism. This decline may result from an accelerated consumption of antioxidant molecules due to increased ROS production, or from impaired biosynthesis and regeneration of these antioxidants, ultimately reflecting a sustained disruption of the tissue's non-enzymatic antioxidant defenses. Similarly, a study conducted by Pereira et al. (2025) reported that exposure of mussel DG tissues to pharmaceutical drugs resulted in a reduction in TAC, thus corroborating our findings. Regarding PFBS, its position close to the glutathione S-transferases (GSTs) vector in the nMDS and higher values in the IBR v2 aligns with a pronounced induction of this group of enzymes in the DG. Glutathione S-transferases represent a key family of phase II detoxification enzymes that catalyze the conjugation of reduced glutathione (GSH) to a variety of electrophilic xenobiotics, facilitating their solubilization and excretion (Mazari et al., 2023; Vaish et al., 2020). The significant upregulation of GSTs activity observed in response to PFBS suggests an intensified cellular effort to detoxify this compound or its potentially reactive metabolites. Although PFBS is a short-chain PFAS often considered less bioaccumulative than its long-chain counterparts, its biochemical impact indicates a capacity to elicit oxidative or electrophilic stress. The activation of GSTs may thus reflect a protective mechanism aimed at preserving redox homeostasis and preventing cellular damage, highlighting the compound's ability to engage cellular defense pathways despite its emerging classification. This is consistent with the findings of Vieira Sanches et al. (2023), who also reported an increase in GSTs activity in the DG of mussels exposed to ionic liquids. In contrast, distinct biochemical effects were observed for PFHxS, particularly evident through the inhibition of GSTs and carboxylesterases (CbEs) activities. These enzymes are crucial components of the detoxification system. Carboxylesterases are a class of phase I detoxification enzymes that play a key role in the hydrolysis of ester-containing xenobiotics and endogenous lipids, contributing to both detoxification and lipid metabolic processes (Solé and Sanchez-Hernandez, 2015). On the other hand, GSTs are phase II detoxification enzymes that catalyze the conjugation of the tripeptide GSH to a wide variety of electrophilic compounds, facilitating their solubilization and excretion. The inhibition of these enzymes indicates a potential impairment of phase I and phase II biotransformation pathways and may reflect the early onset of metabolic disturbance, potentially compromising the body's ability to effectively process and eliminate xenobiotic compounds. A study conducted by Solé and Sanchez-Hernandez (2018) also reported inhibition of CbEs activity following *in vitro* exposure of DG of mussels to human pharmaceuticals and personal care products (PPCPs). Together with the previously noted decrease in TAC, these

findings point toward a compromised cellular defense system, wherein both conjugative detoxification and non-enzymatic antioxidant responses are suppressed. This dual impairment positions PFHxS as a potentially disruptive contaminant capable of undermining multiple biochemical pathways involved in detoxification and redox regulation. The absence of observable cellular damage in the DG following exposure to the emerging PFAS may be attributed to several interrelated factors. Unlike legacy PFAS, these compounds may possess lower bioaccumulative potential, limiting their intracellular concentration and thus reducing their capacity to exert direct cytotoxic effects (Chambers et al., 2021). Additionally, emerging PFAS may exhibit diminished prooxidant activity, thereby generating lower levels of ROS and oxidative stress. Furthermore, despite the observed inhibition of key detoxification enzymes such as CbEs activity and TAC levels, the maintenance of cellular integrity suggests the presence of compensatory or alternative antioxidant pathways. These defense mechanisms may effectively neutralize ROS and mitigate oxidative damage, preserving cellular structure and function even in the face of biochemical disruptions.

Similar to emerging PFAS, exposure to PFOA among the legacy PFAS resulted in increased AChE activity in the DG, suggesting potential disruption of cholinergic pathways or cellular regulatory processes in non-neuronal tissues. This response may reflect an early cellular adaptation to chemical stress, possibly linked to alterations in metabolic or immune-related pathway mechanisms. In contrast, PFOS exposure resulted in a marked increase in lipid peroxidation (LPO) levels, indicating significant oxidative damage likely due to an imbalance in antioxidant defenses. Studies conducted by Liu et al. (2014) also observed that mussels of the *Perna viridis* species exposed to different concentrations (0.1, 1, 10, 100, and 1000 μg/L) of PFOS showed high levels of DNA damage, using the comet assay. High LPO levels were supported by a decrease in CAT activity, suggesting a reduced ability to degrade hydrogen peroxide, thereby contributing to ROS accumulation. At the same time, the increase in CbEs activity may reflect a compensatory detoxification effort in response to PFOS-induced stress, whereas in the case of emerging PFAS, a decrease in CbEs activity was observed, potentially due to different interaction mechanisms with metabolic pathways, which might limit the activation of detoxification processes or indicate a shift in enzymatic regulation in response to these compounds. For instance, following prolonged exposure (7, 14, and 21 days) of *M. galloprovincialis* to PFOS, an increase in GSTs activity in hepatopancreas was observed at 14 and 21 days, suggesting that the duration of exposure influences the temporal dynamics of enzymatic responses (Gülsever and Parlak, 2018). The combination of impaired ROS scavenging (*via* CAT) and increased detoxification activity (*via* CbEs) likely contributes to the elevated LPO levels observed, emphasizing the potent pro-oxidative and membrane-damaging effects of PFOS. In a study carried out by Bi et al. (2022), an increase in malondialdehyde (MDA) levels was observed in the visceral mass of *Corbicula fluminea* following 28 days of exposure to varying concentrations of PFOS, indicating enhanced LPO levels. However, in the present study, PFOS induced oxidative damage at almost all tested concentrations, suggesting that PFOS may have a broader toxicological effect across a range of exposure levels compared to long-chain PFAS and with the emerging ones. On the other hand, PFNA did not induce LPO but, instead, increased the activity of both CAT and CbEs. This combined increase suggests an antioxidant and detoxification response aimed at reducing oxidative stress without causing significant lipid damage. Interestingly, the PFNA profile in the MDS analysis was close to that of the CTL group, indicating a more moderate biochemical effect compared to the other PFAS tested.

Overall, emerging PFAS, including PFBA, GenX, and PFHxS, predominantly result in significant elevations in AChE activity, indicating potential disruption of cholinergic signaling pathways, particularly in non-neuronal tissues such as the DG. These substances also lead to a reduction in TAC, signifying the induction of oxidative stress, although they do not elicit the same degree of oxidative damage as legacy PFAS like PFOS, which promotes increased LPO levels. Emerging PFAS generally activate detoxification enzymes such as GSTs as part of a cellular defense response, while legacy PFAS, especially PFOS, inhibit both GSTs and CbEs activities, suggesting an impairment of detoxification mechanisms. In summary, in the DG, while emerging PFAS appear to induce less oxidative damage, they may still interfere with cellular processes, whereas legacy PFAS, notably PFOS, induce more pronounced toxic effects across multiple biochemical pathways.

4.2.2. Gills

In bivalves, the G perform critical physiological functions, primarily in respiration and filter feeding (Frank et al., 2015; Varotto et al., 2013). Due to their large surface area, dense vascularization and direct, continuous contact with the surrounding aquatic environment, G are a major interface for gas exchange and uptake of suspended particles (Frank et al., 2015; Varotto et al., 2013). These characteristics make them valuable bioindicators in ecotoxicological research as they are particularly susceptible to the accumulation of contaminants of aquatic origin, including trace metals (Liu et al., 2011), rare earth elements (Pinto et al., 2025), pharmaceuticals (Pereira et al., 2025) and persistent organic pollutants such as PFAS (Copeto et al., 2024). Exposure to the emerging PFAS compounds PFBA, GenX and PFHxS resulted in a pronounced inhibition of both TAC levels and CbEs activity in the G tissues. The decrease in TAC reflects a compromised ability to counteract ROS, increasing the risk of oxidative damage, while the suppression of CbEs suggests impaired phase I detoxification. This similar biochemical pattern was already observed in the DG. The parallel disruption of antioxidant defenses and biotransformation pathways in the G and DG highlights a common toxicological profile for PFBA, GenX and PFHxS, suggesting that these emerging PFAS may compromise mussel health by targeting fundamental detoxification and oxidative stress response systems across multiple organs. Studies conducted by Solé and Sanchez-Hernandez (2018) have also observed an inhibition of CbEs in human pharmaceuticals and personal care products, in the G and DG of *M. galloprovincialis*. In particular, after a short exposure to pharmaceuticals in G, Pereira et al. (2025) already observed a reduction in TAC levels. A marked inhibition of AChE activity was consistently observed in the G tissues following exposure to all emerging PFAS, with GenX exhibiting the most pronounced effect. Given the direct exposure of the G to the aquatic environment, the suppression of AChE in this tissue suggests a vulnerability to neurotoxic-like mechanisms potentially triggered by these compounds. AChE in mussel G is thought to play roles beyond classical neurotransmission, including involvement in cell-cell communication, regulation of ion transport and epithelial function. Its inhibition could therefore affect these essential physiological processes and contribute to tissue dysfunction. Studies conducted by Vieira Sanches et al. (2023) also reported a reduction in AChE activity in the G following exposure to ionic liquids. A contrasting response was observed in the DG, where AChE activity increased, particularly in response to PFBA and GenX. This indicates that AChE may be subject to tissue-specific modulation and that its role in mussel physiology may differ. The strong AChE inhibition exhibited by GenX in G tissues underscores its potential for neurotoxicity and suggests a targeted disruption of cholinergic-like signaling at the primary interface of the organism with its environment.

Among legacy PFAS, an intriguing observation pertains to the positioning of PFNA, which is located close to the CTL group on the nMDS for the G tissues, a finding that has previously been observed in the DG. This observation suggests a relatively minor disturbance in the profile of the biomarkers evaluated. However, the biochemical responses reveal specific effects associated with each compound. Notably, both PFOA and PFNA were shown to inhibit SOD activity, indicating a decreased capacity to scavenge superoxide radicals and potentially impairing the organism's primary antioxidant defense mechanism. In contrast, emerging PFAS, particularly PFBA, did not exhibit this inhibitory effect on SOD activity, suggesting a different mechanism of action with respect to antioxidant defense. Similarly, during longer exposure periods (14

days), Pinto et al. (2025) also reported a reduction in SOD activity in mussels G following exposure to different concentrations of the rare earth element yttrium. However, Copeto et al. (2024) reported an increase in SOD activity in *M. galloprovincialis* adults following 28 days of exposure to PFOA, highlighting a potential adaptive antioxidant response over time, however, in the present study, a short-term exposure of 30 min resulted in SOD inhibition, suggesting that antioxidant responses may vary significantly depending on exposure duration. The consistency of these findings, despite differences in exposure duration and contaminant type, indicates that SOD is a sensitive biomarker of oxidative stress in mussels, susceptible to inhibition under both acute and chronic exposure conditions, depending on the nature and intensity of the stressor. Interestingly, similar to GenX, PFNA also induced a significant increase in CAT and CbEs activities, reflecting a comparable response observed in the DG. This suggests a compensatory activation of alternative antioxidant and detoxification pathways in response to the oxidative challenge. Furthermore, among legacy compounds PFOS, PFOA and PFNA consistently suppressed total antioxidant capacity TAC in the G, reflecting a generalized reduction in the tissue's ability to counteract ROS. Pereira et al. (2025) after *in vitro* and *in vivo* experiments observed and inhibition of TAC levels in G of *M. galloprovincialis* exposed to diclofenac and gentamicin. In addition, PFOS and PFNA have been observed to inhibit GSTs, suggesting a possible impairment in phase II detoxification and reduced conjugation of xenobiotics with glutathione. In chronic exposure assays to PFOS lasting 7 (Liu et al., 2020) and 28 days (Bi et al., 2022), a reduction in GSTs activity was also observed in the whole tissue and G, respectively, of *C. fluminea*. Overall, these results suggest that despite their different overall effects as reflected by nMDS aggregation, legacy PFAS exert significant pressure on key enzymatic defenses in the G, disrupting both antioxidant and conjugation functions. However, no significant evidence of cellular damage was detected. This finding suggests that short-term exposure may not be sufficient to induce membrane disruption and raises the possibility that mussels have developed compensatory defense mechanisms capable of mitigating ROS generation or preventing their interaction with membrane lipids. Corroborating these findings, Amraoui et al. (2018) demonstrated that after 7 days exposure to PFOS in the freshwater mussel *Unio ravoisieri* resulted in elevated LPO levels in both tissues (G and DG), indicating oxidative damage after prolonged exposure compared to the present study. Additionally, Xu et al. (2022) observed an increase in LPO levels in the G of the marine mussel *Perna viridis* after 7 days of exposure to varying concentrations of PFOS (10, 100, and 1000 μg/L).

Overall, emerging PFAS (PFBA, GenX, PFHxS) primarily impair antioxidant defenses in G by inhibiting TAC and CbEs activities and suppressing AChE, particularly with GenX, inducing oxidative stress without significant oxidative damage. Conversely, legacy PFAS (PFOS, PFOA, PFNA) cause more pronounced disruptions, including inhibition of SOD, TAC, and GSTs, resulting in oxidative damage. The DG exhibited greater sensitivity, showing broader biochemical alterations such as modulation of AChE, TAC, GSTs, and CbEs activities. Increased AChE activity in the DG following exposure to emerging PFAS suggests disruption of cholinergic signaling, potentially linked to oxidative or metabolic stress. In contrast, G, as the primary environmental interface, showed AChE inhibition and impaired antioxidant defenses but no overt oxidative damage, indicating possible compensatory mechanisms. These results highlight tissue-specific and compound-specific responses, with the DG being the most responsive tissue for biomonitoring PFAS exposure. Similarly, Zhang et al. (2025) emphasize that PFAS toxicity affects both long- and short-chain compounds in invertebrates, underscoring that short-chain PFAS, often regarded as safer alternatives, can still pose significant ecological risks.

4.3. Intra-group variability and ecological implications

An interesting observation from this study was the intra-group variability within the emerging PFAS group, underscoring the limitations of treating them as a homogeneous class. Compounds like GenX and PFBA exhibited highly distinct biochemical profiles compared to PFHxS and PFBS, suggesting divergent modes of action despite structural similarities highlighted by IBR v2 index and nMDS analysis. These findings support the growing consensus that the toxicological behavior of emerging PFAS cannot be generalized and must be evaluated on a compound-specific basis. Similar to our observations, Liu et al. (2023) reported distinct, compound-specific effects of PFOA and GenX on zebrafish development and gene expression. In contrast, legacy PFAS displayed more consistent biochemical responses, particularly in the DG. The clustering of legacy PFAS in the nMDS plots and their relatively uniform IBR v2 values suggest conserved mechanisms of action and predictable toxicokinetics, making these compounds easier to regulate. This consistency, while facilitating regulation, does not diminish their ecological persistence or toxicity. Interestingly, the tissue-specific response patterns highlight the role of organ function in modulating PFAS effects. In the G, legacy PFAS showed more variable responses, whereas PFHxS and PFBS induced more uniform alterations. These contrasting profiles may result from differences in bioavailability, membrane permeability, and tissue-specific enzyme expression.

Overall, the results confirm that legacy PFAS, particularly PFOS, emerged as the most potent disruptors of biochemical homeostasis, exerting strong pro-oxidant effects and broad enzymatic suppression. These patterns are consistent with their known bioaccumulation and toxicity profiles in aquatic organisms (Amraoui et al., 2018; Liu et al., 2014; Xu et al., 2022). Although emerging PFAS such as GenX and PFHxS interfered with key enzymatic systems, they induced less oxidative damage and were often associated with adaptive or reversible responses. However, despite generally subtler effects, they exhibited compound- and tissue-specific disruptions that should not be overlooked. Their capacity to impair detoxification and signaling mechanisms warrants caution, particularly under chronic exposure conditions or in combination with other environmental stressors. These findings support the growing recognition of the need to evaluate the toxicological impacts of emerging PFAS, as emphasized by Wang et al. (2025), who highlight significant knowledge gaps regarding their behavior and effects in marine environments.

5. Conclusion

This study revealed distinct toxicological profiles between legacy and emerging PFAS in *Mytilus galloprovincialis*. Emerging PFAS such as PFBA, GenX, and PFHxS triggered more variable and often stronger biochemical responses, particularly in the digestive gland (DG), including AChE upregulation, antioxidant capacity inhibition, and GSTs or CbEs modulation. Legacy compounds like PFOS and PFOA showed more consistent oxidative stress markers, notably lipid peroxidation and altered enzyme activity. Tissue-specific differences underscore the DG's greater sensitivity compared to the gills (G). Given its broad and sensitive biochemical reactivity, the DG tissues should be prioritized in upcoming environmental monitoring and risk assessment protocols addressing PFAS contamination. Together, these findings underscore the biochemical potency and complexity of emerging PFAS, challenging the perception that newer alternatives are inherently safer. They also highlight the tissue-specific nature of PFAS toxicity and the importance of integrating multiple biomarkers to capture the nuanced effects of these persistent contaminants. The evidence presented reinforces the need for continued ecotoxicological monitoring and regulatory scrutiny of both legacy and emerging PFAS, especially given their environmental persistence and capacity to disrupt critical physiological functions in aquatic organisms.

CRediT authorship contribution statement

Marta Cunha: Writing – review & editing, Writing – original draft,

Visualization, Software, Methodology, Investigation, Formal analysis, Data curation, Conceptualization. **Claudio Bortot:** Formal analysis. **Gianfranco Santovito:** Formal analysis. **Alessandro Nardi:** Writing – review & editing, Validation, Supervision, Investigation, Data curation. **Amadeu M.V.M. Soares:** Resources, Funding acquisition. **Ana M. Gil:** Writing – review & editing, Validation, Supervision, Data curation. **Rosa Freitas:** Writing – review & editing, Visualization, Validation, Supervision, Resources, Investigation, Funding acquisition.

Declaration of competing interest

The authors declare that they have no known competing financial interests or personal relationships that could have appeared to influence the work reported in this paper.

Acknowledgements

Marta Cunha benefited from a PhD grant (2024.01100.BD) funded by National Funds through the Portuguese Science Foundation (Fundação para a Ciência e a Tecnologia, FCT). This work is funded by national funds through FCT – Fundação para a Ciência e a Tecnologia I. P., under the project/grant UID/50006 + LA/P/0094/2020 (doi: 10.54499/LA/P/0094/2020). This work was also developed within the scope of the project CICECO-Aveiro Institute of Materials UIDB/50011/2020 (doi: 10.54499/UIDB/50011/2020), UIDB/50011/2020, UIDP/50011/2020 (doi: 10.54499/UIDP/50011/2020) & LA/P/0006/2020, financed by national funds through the FCT/MCTES (PIDDAC).

Appendix A. Supplementary data

Supplementary data to this article can be found online at https://doi.org/10.1016/j.marpolbul.2025.118490.

Data availability

Data will be made available on request.

References

Ackerman Grunfeld, D., Gilbert, D., Hou, J., Jones, A.M., Lee, M.J., Kibbey, T.C.G., O'Carroll, D.M., 2024. Underestimated burden of per- and polyfluoroalkyl substances in global surface waters and groundwaters. Nat. Geosci. 17 (4), 340–346. https://doi.org/10.1038/s41561-024-01402-8.

Aebi, H., 1984. Catalase *in vitro*. In: Methods in Enzymology, vol. 105. Academic press, pp. 121–126. https://doi.org/10.1016/S0076-6879(84)05016-3.

Alazaiza, M.Y.D., Alzghoul, T.M., Ramu, M.B., Abu Amr, S.S., Abushammala, M.F.M., 2025. PFAS contamination and mitigation: a comprehensive analysis of research trends and global contributions. Case Studies in Chemical and Environmental Engineering 11, 101127. https://doi.org/10.1016/j.cscee.2025.101127.

Amraoui, I., Khalloufi, N., Touaylia, S., 2018. Effects to perfluorooctane sulfonate (PFOS) on the mollusk *Unio ravoisieri* under laboratory exposure. Chem. Ecol. 34 (4), 324–339. https://doi.org/10.1080/02757540.2018.1433168.

An, X., Lei, H., Lu, Y., Xie, X., Wang, P., Liao, J., Liang, Z., Sun, B., Wu, Z., 2023. Per- and polyfluoroalkyl substances (PFASs) in water and sediment from a temperate watershed in China: occurrence, sources, and ecological risks. Sci. Total Environ. 890, 164207. https://doi.org/10.1016/j.scitotenv.2023.164207.

Anderson, M.J., Clarke, K.R., Gorley, R.N., 2008. PERMANOVA+ for PRIMER: Guide to Software and Statistical Methods. Primer-E.

Apelberg, B.J., Witter, F.R., Herbstman, J.B., Calafat, A.M., Halden, R.U., Needham, L.L., Goldman, L.R., 2007. Cord serum concentrations of perfluorooctane sulfonate (PFOS) and perfluorooctanoate (PFOA) in relation to weight and size at birth. Environ. Health Perspect. 115 (11), 1670–1676. https://doi.org/10.1289/ehp.10334.

Ateia, M., Maroli, A., Tharayil, N., Karanfil, T., 2019. The overlooked short- and ultrashort-chain poly- and perfluorinated substances: a review. Chemosphere 220, 866–882. https://doi.org/10.1016/j.chemosphere.2018.12.186.

Australia, S.C., 2024. Addendum to PFAS evidence evaluation for Australian drinking water guidelines chemical fact sheets. SLR Project No.: 640.031365.00001. National Health and Medical Research Council. October 17, 2024. https://www.nhmrc.gov.au/sites/default/files/documents/attachments/water-PFAS/Addendum-to-PFAS-Report.pdf.

Bangma, J., Guillette, T.C., Bommarito, P.A., Ng, C., Reiner, J.L., Lindstrom, A.B., Strynar, M.J., 2022. Understanding the dynamics of physiological changes, protein expression, and PFAS in wildlife. Environ. Int. 159, 107037. https://doi.org/10.1016/j.envint.2021.107037.

Beliaeff, B., Burgeot, T., 2002. Integrated biomarker response: a useful tool for ecological risk assessment. Environ. Toxicol. Chem. 21 (6), 1316–1322.

Benzie, I.F.F., Strain, J.J., 1996. The ferric reducing ability of plasma (FRAP) as a measure of "antioxidant power": the FRAP assay. Anal. Biochem. 239 (1), 70–76. https://doi.org/10.1006/abio.1996.0292.

Bernardini, I., Matozzo, V., Valsecchi, S., Peruzza, L., Rovere, G.D., Polesello, S., Iori, S., Marin, M.G., Fabrello, J., Ciscato, M., Masiero, L., Bonato, M., Santovito, G., Boffo, L., Bargelloni, L., Milan, M., Patarnello, T., 2021. The new PFAS C6O4 and its effects on marine invertebrates: first evidence of transcriptional and microbiota changes in the Manila clam *Ruditapes philippinarum*. Environ. Int. 152. https://doi.org/10.1016/j.envint.2021.106484.

Bi, C., Junaid, M., Liu, Y., Guo, W., Jiang, X., Pan, B., Li, Z., Xu, N., 2022. Graphene oxide chronic exposure enhanced perfluorooctane sulfonate mediated toxicity through oxidative stress generation in freshwater clam *Corbicula fluminea*. Chemosphere 297, 134242. https://doi.org/10.1016/j.chemosphere.2022.134242.

Boiteux, V., Dauchy, X., Bach, C., Colin, A., Hemard, J., Sagres, V., Rosin, C., Munoz, J.-F., 2017. Concentrations and patterns of perfluoroalkyl and polyfluoroalkyl substances in a river and three drinking water treatment plants near and far from a major production source. Sci. Total Environ. 583, 393–400. https://doi.org/10.1016/j.scitotenv.2017.01.079.

Bonato, M., Corrà, F., Bellio, M., Guidolin, L., Tallandini, L., Irato, P., Santovito, G., 2020. PFAS environmental pollution and antioxidant responses: an overview of the impact on human field. Int. J. Environ. Res. Public Health 17 (21), 8020. https://doi.org/10.3390/ijerph17218020.

Brendel, S., Fetter, É., Staude, C., Vierke, L., Biegel-Engler, A., 2018. Short-chain perfluoroalkyl acids: environmental concerns and a regulatory strategy under REACH. Environmental sciences. Europe 30 (1). https://doi.org/10.1186/s12302-018-0134-4.

Brusseau, M.L., Anderson, R.H., Guo, B., 2020. PFAS concentrations in soils: background levels versus contaminated sites. Sci. Total Environ. 740, 140017. https://doi.org/10.1016/j.scitotenv.2020.140017.

Brusseau, M.L., Guo, B., 2022. PFAS concentrations in soil versus soil porewater: mass distributions and the impact of adsorption at air-water interfaces. Chemosphere 302, 134938. https://doi.org/10.1016/j.chemosphere.2022.134938.

Buck, R.C., Franklin, J., Berger, U., Conder, J.M., Cousins, I.T., Voogt, P., De Jensen, A. A., Kannan, K., Mabury, S.A., van Leeuwen, S.P.J., 2011. Perfluoroalkyl and polyfluoroalkyl substances in the environment: terminology, classification, and origins. Integr. Environ. Assess. Manag. 7 (4), 513–541. https://doi.org/10.1002/ieam.258.

Cai, M., Zhao, Z., Yin, Z., Ahrens, L., Huang, P., Cai, M., Yang, H., He, J., Sturm, R., Ebinghaus, R., Xie, Z., 2012. Occurrence of perfluoroalkyl compounds in surface waters from the North Pacific to the Arctic Ocean. Environ. Sci. Technol. 46 (2), 661–668. https://doi.org/10.1021/es2026278.

Carregosa, V., Velez, C., Pires, A., Soares, A., Figueira, E., Freitas, R., 2014. Physiological and biochemical responses of the Polychaete *Diopatra neapolitana* to organic matter enrichment. Aquat. Toxicol. 155C, 32–42. https://doi.org/10.1016/j.aquatox.2014.05.029.

Chahouri, A., Yacoubi, B., Moukrim, A., Banaoui, A., 2023. Bivalve molluscs as bioindicators of multiple stressors in the marine environment: recent advances. Cont. Shelf Res. 264, 105056. https://doi.org/10.1016/j.csr.2023.105056.

Chambers, W.S., Hopkins, J.G., Richards, S.M., 2021. A review of per- and Polyfluorinated alkyl substance impairment of reproduction. Frontiers in Toxicology 3. https://doi.org/10.3389/ftox.2021.732436.

Chen, H., Sun, R., Zhang, C., Han, J., Wang, X., Han, G., He, X., 2016. Occurrence, spatial and temporal distributions of perfluoroalkyl substances in wastewater, seawater and sediment from Bohai Sea, China. Environ. Pollut. 219, 389–398. https://doi.org/10.1016/j.envpol.2016.05.017.

Chiarelli, R., Roccheri, M., 2014. Marine invertebrates as bioindicators of heavy metal pollution. Open Journal of Metal 04, 93–106. https://doi.org/10.4236/ojmetal.2014.44011.

Clarke, K.R., Warwick, R.M., Marine, P., 2001. CHANGE IN MARINE COMMUNITIES An Approach to Statistical Analysis and Interpretation, 2nd edition.

Copeto, S., Gonçalo, S., Ferreira, I.J., Sanchez, D., Nunes, M.J., Motta, C., Silva, M., Diniz, M., 2024. The impact of Perfluorooctanoic acid (PFOA) on the mussel *Mytilus galloprovincialis*: a multi-biomarker evaluation. Oceans 5 (4), 857–873. https://doi.org/10.3390/oceans5040049.

Cousins, I.T., Ng, C.A., Wang, Z., Scheringer, M., 2019. Why is high persistence alone a major cause of concern? Environ Sci Process Impacts 21 (5), 781–792. https://doi.org/10.1039/c8em00515j.

Crone, B.C., Speth, T.F., Wahman, D.G., Smith, S.J., Abulikemu, G., Kleiner, E.J., Pressman, J.G., 2019. Occurrence of per- and polyfluoroalkyl substances (PFAS) in source water and their treatment in drinking water. Crit. Rev. Environ. Sci. Technol. 49 (24), 2359–2396. https://doi.org/10.1080/10643389.2019.1614848.

Cruz, P., Cuccaro, A., Pretti, C., He, Y., Soares, A.M.V.M., Freitas, R., 2023. Comparative subcellular responses to pharmaceutical exposures in the mussel *Mytilus galloprovincialis*: An *in vitro* study. Environ. Toxicol. Pharmacol. 104. https://doi.org/10.1016/j.etap.2023.104314.

Cunha, I., Hoff, P., Van de Vijver, K., Guilhermino, L., Esmans, E., De Coen, W., 2005. Baseline study of perfluorooctane sulfonate occurrence in mussels, *Mytilus galloprovincialis*, from north-central portuguese estuaries. Mar. Pollut. Bull. 50 (10), 1128–1132. https://doi.org/10.1016/j.marpolbul.2005.06.046.

Dasu, K., Xia, X., Siriwardena, D., Klupinski, T.P., Seay, B., 2022. Concentration profiles of per- and polyfluoroalkyl substances in major sources to the environment. J. Environ. Manag. 301, 113879. https://doi.org/10.1016/j.jenvman.2021.113879.

Dean, W.S., Adejumo, H.A., Caiati, A., Garay, P.M., Harmata, A.S., Li, L., Sundar, S., 2020. A framework for regulation of new and existing PFAS by EPA. Journal of Science Policy & Governance 16 (1), 1–14.

Dettori, M., Arghittu, A., Deiana, G., Castiglia, P., Azara, A., 2022. The revised European directive 2020/2184 on the quality of water intended for human consumption. A step forward in risk assessment, consumer safety and informative communication. Environ. Res. 209, 112773. https://doi.org/10.1016/j.envres.2022.112773.

Du, Z., Deng, S., Chen, Y., Wang, B., Huang, J., Wang, Y., Yu, G., 2015. Removal of perfluorinated carboxylates from washing wastewater of perfluorooctanesulfonyl fluoride using activated carbons and resins. J. Hazard. Mater. 286, 136–143. https://doi.org/10.1016/j.jhazmat.2014.12.037.

ECHA, 2024. European chemicals agency. Annu. Rep. 2024. https://echa.europa.eu/annual-report-2024. (Accessed 22 April 2025).

EFSA, 2008. Perfluorooctane sulfonate (PFOS), perfluorooctanoic acid (PFOA) and their salts scientific opinion of the panel on contaminants in the food chain. EFSA J. 6, 653.

Ellman, G.L., Courtney, K.D., Andres, V., Featherstone, R.M., 1961. A new and rapid colorimetric determination of acetylcholinesterase activity. Biochem. Pharmacol. 7 (2), 88–95. https://doi.org/10.1016/0006-2952(61)90145-9.

European Commission, 2024. Commission notice – Technical guidelines regarding methods of analysis for monitoring of per- and polyfluoroalkyl substances (PFAS) in water intended for human consumption (C/2024/5414). https://eur-lex.europa.eu/eli/C/2024/4910/oj accessed 22 April 2025.

Evich, M.G., Davis, M.J.B., McCord, J.P., Acrey, B., Awkerman, J.A., Knappe, D.R.U., Lindstrom, A.B., Speth, T.F., Tebes-Stevens, C., Strynar, M.J., Wang, Z., Weber, E.J., Henderson, W.M., Washington, J.W., 2025. Per- and polyfluoroalkyl substances in the environment. Science 375 (6580), eabg9065. https://doi.org/10.1126/science.abg9065.

Fabbri, R., Montagna, M., Balbi, T., Raffo, E., Palumbo, F., Canesi, L., 2014. Adaptation of the bivalve embryotoxicity assay for the high-throughput screening of emerging contaminants in *Mytilus galloprovincialis*. Mar. Environ. Res. 99, 1–8. https://doi.org/10.1016/j.marenvres.2014.05.007.

Faggio, C., Tsarpali, V., Dailianis, S., 2018. Mussel digestive gland as a model tissue for assessing xenobiotics: An overview. Sci. Total Environ. 636, 220–229. https://doi.org/10.1016/j.scitotenv.2018.04.264.

Fair, P.A., Wolf, B., White, N.D., Arnott, S.A., Kannan, K., Karthikraj, R., Vena, J.E., 2019. Perfluoroalkyl substances (PFASs) in edible fish species from Charleston Harbor and tributaries, South Carolina, United States: exposure and risk assessment. Environ. Res. 171, 266–277. https://doi.org/10.1016/j.envres.2019.01.021.

Frank, D.M., Deaton, L., Shumway, S.E., Holohan, B.A., Ward, J.E., 2015. Modulation of pumping rate by two species of marine bivalve molluscs in response to neurotransmitters: comparison of *in vitro* and *in vivo* results. Comparative Biochemistry and Physiology -Part A : Molecular and Integrative Physiology 185, 150–158. https://doi.org/10.1016/j.cbpa.2015.03.015.

Gaines, L.G., 2023. Historical and current usage of per-and polyfluoroalkyl substances (PFAS): a literature review. Am. J. Ind. Med. 66 (5), 353–378. https://doi.org/10.1002/ajim.23362.

Gellrich, V., Brunn, H., Stahl, T., 2013. Perfluoroalkyl and polyfluoroalkyl substances (PFASs) in mineral water and tap water. Journal of Environmental Science and Health - Part A Toxic/Hazardous Substances and Environmental Engineering 48 (2), 129–135. https://doi.org/10.1080/10934529.2013.719431.

Gewurtz, S.B., Bradley, L.E., Backus, S., Dove, A., McGoldrick, D., Hung, H., Dryfhout-Clark, H., 2019. Perfluoroalkyl acids in Great Lakes precipitation and surface water (2006-2018) indicate response to phase-outs, regulatory action, and variability in fate and transport processes. Environ. Sci. Technol. 53 (15), 8543–8552. https://doi.org/10.1021/acs.est.9b01337.

Giannessi, J., De Marchi, L., Meucci, V., Intorre, L., Monni, G., Baratti, M., Pretti, C., 2023. Subcellular tissue-specific responses of *Mytilus galloprovincialis* to fluoroquinolone antibiotics. Environ. Toxicol. Pharmacol. 104, 104306. https://doi.org/10.1016/j.etap.2023.104306.

Giari, L., Guerranti, C., Perra, G., Cincinelli, A., Gavioli, A., Lanzoni, M., Castaldelli, G., 2023. PFAS levels in fish species in the Po River (Italy): new generation PFAS, fish ecological traits and parasitism in the foreground. Sci. Total Environ. 876, 162828. https://doi.org/10.1016/j.scitotenv.2023.162828.

Glenn, G., Shogren, R., Jin, X., Orts, W., Hart-Cooper, W., Olson, L., 2021. Per- and polyfluoroalkyl substances and their alternatives in paper food packaging. Compr. Rev. Food Sci. Food Saf. 20 (3), 2596–2625. https://doi.org/10.1111/1541-4337.12726.

Göckener, B., Weber, T., Rüdel, H., Bücking, M., Kolossa-Gehring, M., 2020. Human biomonitoring of per- and polyfluoroalkyl substances in German blood plasma samples from 1982 to 2019. Environ. Int. 145, 106123. https://doi.org/10.1016/j.envint.2020.106123.

Good, S., Charbonnet, J.A., 2024. Extractable per- and Polyfluoroalkyl substances in menstrual underwear. Environ. Eng. Sci. https://doi.org/10.1089/ees.2024.0270.

Gülsever, G., Parlak, H., 2018. Effects of Perfluorooctane sulfonate compounds on the biochemical activities in mussels (*Mytilus galloprovincialis*). Ege Journal of Fisheries and Aquatic Sciences 35 (4), 417–422. https://doi.org/10.12714/egejfas.2018.35.4.07.

Habig, W.H., Pabst, M.J., Jakoby, W.B., 1974. Glutathione S-transferases: the first enzymatic step in mercapturic acid formation. J. Biol. Chem. 249 (22), 7130–7139. https://doi.org/10.1016/S0021-9258(19)42083-8.

Hagger, J.A., Depledge, M.H., Galloway, T.S., 2005. Toxicity of tributyltin in the marine mollusc *Mytilus edulis*. Mar. Pollut. Bull. 51 (8–12), 811–816. https://doi.org/10.1016/j.marpolbul.2005.06.044.

Heo, J.J., Lee, J.W., Kim, S.K., Oh, J.E., 2014. Foodstuff analyses show that seafood and water are major perfluoroalkyl acids (PFAAs) sources to humans in Korea. J. Hazard. Mater. 279, 402–409. https://doi.org/10.1016/j.jhazmat.2014.07.004.

Hosokawa, M., Satoh, T., 2001. Measurement of carboxylesterase (CES) activities. Current protocols. Toxicology 10 (1). https://doi.org/10.1002/0471140856.tx0407s10, 4.7.1-4.7.14.

Hung, M.D., Jung, H.J., Jeong, H.H., Lam, N.H., Cho, H.S., 2020. Perfluoroalkyl substances (PFASs) in special management sea areas of Korea: distribution and bioconcentration in edible fish species. Mar. Pollut. Bull. 156, 111236. https://doi.org/10.1016/j.marpolbul.2020.111236.

Kanduč, T., Medaković, D., Hamer, B., 2011. *Mytilus galloprovincialis* as a bioindicator of environmental conditions: the case of the eastern coast of the Adriatic Sea. Isot. Environ. Health Stud. 47 (1), 42–61. https://doi.org/10.1080/10256016.2011.548866.

Knutsen, H.K., Alexander, J., Barregård, L., Bignami, M., Brüschweiler, B., Ceccatelli, S., Cottrill, B., Dinovi, M., Edler, L., Grasl-Kraupp, B., Hogstrand, C., Hoogenboom . Ron,), L., Nebbia, C.S., Oswald, I.P., Petersen, A., Rose, M., Roudot, A.-C., Vleminckx, C., Vollmer, G., Wallace, H., Bodin, L., Cravedi, J.-P., Halldorsson, T.I., Haug, L.S., Johansson, N., Loveren, H., van Gergelova, P., Mackay, K., Levorato, S., Manen, M., van Schwerdtle, T., 2018. Risk to human health related to the presence of perfluorooctane sulfonic acid and perfluorooctanoic acid in food. EFSA J. 16.

Kurwadkar, S., Dane, J., Kanel, S.R., Nadagouda, M.N., Cawdrey, R.W., Ambade, B., Struckhoff, G.C., Wilkin, R., 2022. Per- and polyfluoroalkyl substances in water and wastewater: a critical review of their global occurrence and distribution. Sci. Total Environ. 809, 151003. https://doi.org/10.1016/j.scitotenv.2021.151003.

Li, F., Duan, J., Tian, S., Ji, H., Zhu, Y., Wei, Z., Zhao, D., 2020. Short-chain per-and polyfluoroalkyl substances in aquatic systems: occurrence, impacts and treatment. Chem. Eng. J. 380, 122506. https://doi.org/10.1016/j.cej.2019.122506.

Li, N., Ying, G.G., Hong, H., Deng, W.J., 2021. Perfluoroalkyl substances in the urine and hair of preschool children, airborne particles in kindergartens, and drinking water in Hong Kong. Environ. Pollut. 270. https://doi.org/10.1016/j.envpol.2020.116219.

Li, X., Shen, X., Jiang, W., Xi, Y., Li, S., 2024. Comprehensive review of emerging contaminants: detection technologies, environmental impact, and management strategies. Ecotoxicol. Environ. Saf. 278, 116420. https://doi.org/10.1016/j.ecoenv.2024.116420.

Liu, C., Gin, K.Y., 2018. Immunotoxicity in green mussels under perfluoroalkyl substance (PFAS) exposure: reversible response and response model development. Environ. Toxicol. Chem. 37 (4), 1138–1145. https://doi.org/10.1002/etc.4060.

Liu, C., Gin, K.Y.H., Chang, V.W.C., 2014. Multi-biomarker responses in green mussels exposed to PFCs: effects at molecular, cellular, and physiological levels. Environ. Sci. Pollut. Res. 21 (4), 2785–2794. https://doi.org/10.1007/s11356-013-2216-6.

Liu, H., Chen, Y., Hu, W., Luo, Y., Zhu, P., You, S., Li, Y., Jiang, Z., Wu, X., Li, X., 2023. Impacts of PFOAC8, GenXC6, and their mixtures on zebrafish developmental toxicity and gene expression provide insight about tumor-related disease. Sci. Total Environ. 858, 160085. https://doi.org/10.1016/j.scitotenv.2022.160085.

Liu, X., Zhang, L., You, L., Yu, J., Zhao, J., Li, L., Wang, Q., Li, F., Li, C., Liu, D., Wu, H., 2011. Differential toxicological effects induced by mercury in gills from three pedigrees of Manila clam *Ruditapes philippinarum* by NMR-based metabolomics. Ecotoxicology 20 (1), 177–186. https://doi.org/10.1007/s10646-010-0569-x.

Liu, Y., Junaid, M., Xu, P., Zhong, W., Pan, B., Xu, N., 2020. Suspended sediment exacerbates perfluorooctane sulfonate mediated toxicity through reactive oxygen species generation in freshwater clam *Corbicula fluminea*. Environ. Pollut. 267. https://doi.org/10.1016/j.envpol.2020.115671.

Lorenzo, M., Campo, J., Farré, M., Pérez, F., Picó, Y., Barceló, D., 2016. Perfluoroalkyl substances in the Ebro and Guadalquivir river basins (Spain). Sci. Total Environ. 540, 191–199. https://doi.org/10.1016/j.scitotenv.2015.07.045.

Magnani, L., Gaydou, E.M., Hubaud, J.C., 2000. Spectrophotometric measurement of antioxidant properties of flavones and flavonols against superoxide anion. Anal. Chim. Acta 411 (1–2), 209–216. https://doi.org/10.1016/S0003-2670(00)00717-0.

Malik, P., Nandini, D., Tripathi, B.P., 2024. Firefighting aqueous film forming foam composition, properties and toxicity: a review. Environ. Chem. Lett. 22 (4), 2013–2033. https://doi.org/10.1007/s10311-024-01739-x.

Manojkumar, Y., Pilli, S., Rao, P.V., Tyagi, R.D., 2023. Sources, occurrence and toxic effects of emerging per- and polyfluoroalkyl substances (PFAS). Neurotoxicol. Teratol. 97, 107174. https://doi.org/10.1016/j.ntt.2023.107174.

Mazari, A.M., Zhang, L., Ye, Z.W., Zhang, J., Tew, K.D., Townsend, D.M., 2023. The multifaceted role of glutathione S-transferases in health and disease. Biomolecules 13 (4), 688. https://doi.org/10.3390/biom13040688.

Mennillo, E., Casu, V., Tardelli, F., De Marchi, L., Freitas, R., Pretti, C., 2017. Suitability of cholinesterase of polychaete *Diopatra neapolitana* as biomarker of exposure to pesticides: *in vitro* characterization. Comp. Biochem. Physiol., Part C: Toxicol. Pharmacol. 191, 152–159. https://doi.org/10.1016/j.cbpc.2016.10.007.

Möller, A., Ahrens, L., Surm, R., Westerveld, J., van der Wielen, F., Ebinghaus, R., de Voogt, P., 2010. Distribution and sources of polyfluoroalkyl substances (PFAS) in the river Rhine watershed. Environ. Pollut. 158 (10), 3243–3250. https://doi.org/10.1016/j.envpol.2010.07.019.

Muir, D., Miaz, L.T., 2021. Spatial and temporal trends of Perfluoroalkyl substances in Global Ocean and coastal waters. Environ. Sci. Technol. 55 (14), 9527–9537. https://doi.org/10.1021/acs.est.0c08035.

Mumtaz, M., Bao, Y., Liu, L., Huang, J., Cagnetta, G., Yu, G., 2019. Per- and Polyfluoroalkyl substances in representative fluorocarbon surfactants used in Chinese film-forming foams: levels, profile shift, and environmental implications. Environmental Science and Technology Letters 6 (5), 259–264. https://doi.org/10.1021/acs.estlett.9b00154.

Ng, C., Cousins, I.T., DeWitt, J.C., Glüge, J., Goldenman, G., Herzke, D., Wang, Z., 2021. Addressing urgent questions for PFAS in the 21st century. Environ. Sci. Technol. 55 (19), 12755–12765. https://doi.org/10.1021/acs.est.1c03386.

OECD, 2018. Summary report on the new comprehensive global database of per- and Polyfluoroalkyl substances (PFASs). OECD Series on Risk Management of Chemicals, OECD Publishing. https://doi.org/10.1787/1a14ad6c-en. Paris.

OECD, 2019. Guidance document on aquatic toxicity testing of difficult substances and mixtures. OECD Series on Testing and Assessment, OECD Publishing. https://doi.org/10.1787/0ed2f88e-en. Paris.

Ohkawa, H., Ohishi, N., Yagi, K., 1979. Assay for lipid peroxides in animal tissues by thiobarbituric acid reaction. Anal. Biochem. 95 (2), 351–358. https://doi.org/10.1016/0003-2697(79)90738-3.

Olsen, G.W., Burris, J.M., Ehresman, D.J., Froelich, J.W., Seacat, A.M., Butenhoff, J.L., Zobel, L.R., 2007. Half-life of serum elimination of perfluorooctanesulfonate, perfluorohexanesulfonate, and perfluorooctanoate in retired fluorochemical production workers. Environ. Health Perspect. 115 (9), 1298–1305. https://doi.org/10.1289/ehp.10009.

Olsen, G.W., Chang, S.C., Noker, P.E., Gorman, G.S., Ehresman, D.J., Lieder, P.H., Butenhoff, J.L., 2009. A comparison of the pharmacokinetics of perfluorobutanesulfonate (PFBS) in rats, monkeys, and humans. Toxicology 256 (1–2), 65–74. https://doi.org/10.1016/j.tox.2008.11.008.

Paige, T., De Silva, T., Buddhadasa, S., Prasad, S., Nugegoda, D., Pettigrove, V., 2024. Background concentrations and spatial distribution of PFAS in surface waters and sediments of the greater Melbourne area. Australia. Chemosphere 349, 140791. https://doi.org/10.1016/j.chemosphere.2023.140791.

Pelch, K.E., Reade, A., Wolffe, T.A., Kwiatkowski, C.F., 2019. PFAS health effects database: protocol for a systematic evidence map. Environ. Int. 130, 104851. https://doi.org/10.1016/j.envint.2019.05.045.

Pereira, A., Cunha, M., Cuccaro, A., Vieira, H.C., He, Y., Soares, A.M.V.M., Freitas, R., 2025. The ecotoxicological effects of diclofenac and gentamicin on *Mytilus galloprovincialis*: what does *in vivo* reveal that in vitro fails to show? Environ. Pollut. 372. https://doi.org/10.1016/j.envpol.2025.126045.

Pétré, M.-A., Salk, K.R., Stapleton, H.M., Ferguson, P.L., Tait, G., Obenour, D.R., Knappe, D.R.U., Genereux, D.P., 2022. Per- and polyfluoroalkyl substances (PFAS) in river discharge: modeling loads upstream and downstream of a PFAS manufacturing plant in the cape fear watershed, North Carolina. Sci. Total Environ. 831, 154763. https://doi.org/10.1016/j.scitotenv.2022.154763.

Pinto, J., Cunha, M., Leite, C., Soares, A.M.V.M., Freitas, R., Pereira, E., 2025. Investigating the effects of anthropogenic yttrium contamination: biochemical alterations in the gills and digestive gland of exposed mussels (*Mytilus galloprovincialis*). Environ. Toxicol. Pharmacol. 114, 104650. https://doi.org/10.1016/j.etap.2025.104650.

Podder, A., Sadmani, A.A., Reinhart, D., Chang, N.B., Goel, R., 2021. Per and poly-fluoroalkyl substances (PFAS) as a contaminant of emerging concern in surface water: a transboundary review of their occurrences and toxicity effects. J. Hazard. Mater. 419, 126361. https://doi.org/10.1016/j.jhazmat.2021.126361.

Poothong, S., Papadopoulou, E., Padilla-Sánchez, J.A., Thomsen, C., Haug, L.S., 2020. Multiple pathways of human exposure to poly- and perfluoroalkyl substances (PFASs): from external exposure to human blood. Environ. Int. 134, 105244. https://doi.org/10.1016/j.envint.2019.105244.

Robinson, H.W., Hogden, C.G., 1940. The biuret reaction in the determination of serum proteins. 1. A study of the conditions necessary for the production of a stable color which bears a quantitative relationship to the protein concentration. J. Biol. Chem. 135 (2), 707–725. https://doi.org/10.1016/S0021-9258(18)73134-7.

Sanchez, W., Burgeot, T., Porcher, J.-M., 2013. A novel "integrated biomarker response" calculation based on reference deviation concept. Environ. Sci. Pollut. Res. Int. 20 (5), 2721–2725. https://doi.org/10.1007/s11356-012-1359-1.

Schrenk, D., Bignami, M., Bodin, L., Chipman, J.K., del Mazo, J., Grasl-Kraupp, B., Hogstrand, C., Hoogenboom, L., Leblanc, J.C., Nebbia, C.S., Nielsen, E., Ntzani, E., Petersen, A., Sand, S., Vleminckx, C., Wallace, H., Barregård, L., Ceccatelli, S., Cravedi, J.P., Schwerdtle, T., 2020. Risk to human health related to the presence of perfluoroalkyl substances in food. EFSA J. 18 (9). https://doi.org/10.2903/j.efsa.2020.6223.

Schwanz, T.G., Llorca, M., Farré, M., Barceló, D., 2016. Perfluoroalkyl substances assessment in drinking waters from Brazil, France and Spain. Sci. Total Environ. 539, 143–152. https://doi.org/10.1016/j.scitotenv.2015.08.034.

Shao, M., Ding, G., Zhang, J., Wei, L., Xue, H., Zhang, N., Li, Y., Chen, G., Sun, Y., 2016. Occurrence and distribution of perfluoroalkyl substances (PFASs) in surface water and bottom water of the Shuangtaizi estuary, China. Environ. Pollut. 216, 675–681. https://doi.org/10.1016/j.envpol.2016.06.031.

Sinclair, G.M., Long, S.M., Jones, O.A.H., 2020. What are the effects of PFAS exposure at environmentally relevant concentrations? Chemosphere 258, 127340. https://doi.org/10.1016/j.chemosphere.2020.127340.

Solé, M., Rivera-Ingraham, G., Freitas, R., 2018. The use of carboxylesterases as biomarkers of pesticide exposure in bivalves: a methodological approach. Comparative Biochemistry and Physiology Part - C: Toxicology and Pharmacology 212 (March), 18–24. https://doi.org/10.1016/j.cbpc.2018.06.002.

Solé, M., Sanchez-Hernandez, J.C., 2015. An *in vitro* screening with emerging contaminants reveals inhibition of carboxylesterase activity in aquatic organisms. Aquat. Toxicol. 169, 215–222. https://doi.org/10.1016/j.aquatox.2015.11.001.

Solé, M., Sanchez-Hernandez, J.C., 2018. Elucidating the importance of mussel carboxylesterase activity as exposure biomarker of environmental contaminants of current concern: An *in vitro* study. Ecol. Indic. 85, 432–439. https://doi.org/10.1016/j.ecolind.2017.10.046.

Sörengård, M., Bergström, S., McCleaf, P., Wiberg, K., Ahrens, L., 2022. Long-distance transport of per- and polyfluoroalkyl substances (PFAS) in a Swedish drinking water aquifer. Environ. Pollut. 311, 119981. https://doi.org/10.1016/j.envpol.2022.119981.

Sun, M., Arevalo, E., Strynar, M., Lindstrom, A., Richardson, M., Kearns, B., Pickett, A., Smith, C., Knappe, D.R.U., 2016. Legacy and emerging Perfluoroalkyl substances are important drinking water contaminants in the cape fear river watershed of North Carolina. Environmental Science and Technology Letters 3 (12), 415–419. https://doi.org/10.1021/acs.estlett.6b00398.

Tresnakova, N., Famulari, S., Zicarelli, G., Impellitteri, F., Pagano, M., Presti, G., Filice, M., Caferro, A., Gulotta, E., Salvatore, G., Sandova, M., Vazzana, I., Imbrogno, S., Capillo, G., Savoca, S., Velisek, J., Faggio, C., 2023. Multi-characteristic toxicity of enantioselective chiral fungicide tebuconazole to a model organism Mediterranean mussel *Mytilus galloprovincialis* Lamarck, 1819 (bivalve: Mytilidae). Sci. Total Environ. 862. https://doi.org/10.1016/j.scitotenv.2022.160874.

USEPA, 2022. U.S. Environmental Protection Agency. PFAS structure list (PFASSTRUCT). https://comptox.epa.gov/dashboard/chemical-lists/PFASSTRUCT. (Accessed 22 April 2025).

USEPA, 2024. U.S. Environmental Protection Agency. Final PFAS national primary drinking water regulation. https://www.epa.gov/sdwa/and-polyfluoroalkyl-substances-pfas. (Accessed 22 April 2025).

Vaish, S., Gupta, D., Mehrotra, R., Mehrotra, S., Basantani, M.K., 2020. Glutathione S-transferase: a versatile protein family. 3. Biotech 10, 1–19. https://doi.org/10.1007/s13205-020-02312-3.

Varotto, L., Domeneghetti, S., Rosani, U., Manfrin, C., Cajaraville, M.P., Raccanelli, S., Pallavicini, A., Venier, P., 2013. DNA damage and transcriptional changes in the gills of *Mytilus galloprovincialis* exposed to Nanomolar doses of combined metal salts (cd, cu, hg). PLoS One 8 (1). https://doi.org/10.1371/journal.pone.0054602.

Vieira Sanches, M., Oliva, M., Mezzetta, A., Guazzelli, L., De Marchi, L., Freitas, R., Pretti, C., 2023. *In vitro* screening of imidazolium and pyrrolidinium based ionic liquids toxicity on subcellular fractions of the Mediterranean mussel *Mytilus galloprovincialis*. Environ. Toxicol. Pharmacol. 104. https://doi.org/10.1016/j.etap.2023.104305.

Wang, Q., Shao, Y., Leung, K.M.Y., Lam, P.K.S., Ruan, Y., 2025. Per- and polyfluoroalkyl substances (PFAS) in the marine environment: An overview and prospects. Mar. Pollut. Bull. 216. https://doi.org/10.1016/j.marpolbul.2025.117993.

Wang, Q., Tsui, M.M.P., Ruan, Y., Lin, H., Zhao, Z., Ku, J.P.H., Sun, H., Lam, P.K.S., 2019. Occurrence and distribution of per- and polyfluoroalkyl substances (PFASs) in the seawater and sediment of the South China Sea coastal region. Chemosphere 231, 468–477. https://doi.org/10.1016/j.chemosphere.2019.05.162.

Wang, X., Lv, Y., Qiang, X., Liang, S., Li, R., Zhan, J., Liu, J., 2024. Perfluorooctanoic acid (PFOA) and its alternative perfluorobutanoic acid (PFBA) alter hepatic bile acid profiles via different pathways. Sci. Total Environ. 950. https://doi.org/10.1016/j.scitotenv.2024.175312.

Wang, Z., Dewitt, J.C., Higgins, C.P., Cousins, I.T., 2017. A never-ending story of per- and Polyfluoroalkyl substances (PFASs)? Environ. Sci. Technol. 51 (5), 2508–2518. https://doi.org/10.1021/acs.est.6b04806.

Whitehead, H.D., Venier, M., Wu, Y., Eastman, E., Urbanik, S., Diamond, M.L., Shalin, A., Schwartz-Narbonne, H., Bruton, T.A., Blum, A., Wang, Z., Green, M., Tighe, M., Wilkinson, J.T., McGuinness, S., Peaslee, G.F., 2021. Fluorinated compounds in north American cosmetics. Environmental Science and Technology Letters 8 (7), 538–544. https://doi.org/10.1021/acs.estlett.1c00240.

Wicks, A., Whitehead, H.D., Peaslee, G.F., 2024. Presence of Perfluorohexanoic acid in Fluoroelastomer watch bands. Environ. Sci. Technol. Lett. 12 (1), 25–30. https://doi.org/10.1021/acs.estlett.4c00907.

Xu, P., Junaid, M., Liu, Y., Jiang, X., Chen, Y., Bi, C., Wang, J., Xu, N., 2022. Nanoplastics influence the perfluorooctane sulfonate (PFOS) mediated toxicity on marine mussel *Perna viridis*: single and mixture exposure study. Gondwana Res. 108, 144–157. https://doi.org/10.1016/j.gr.2021.12.001.

Yan, H., Zhang, C.J., Zhou, Q., Chen, L., Meng, X.Z., 2012. Short- and long-chain perfluorinated acids in sewage sludge from Shanghai. China. Chemosphere 88 (11), 1300–1305. https://doi.org/10.1016/j.chemosphere.2012.03.105.

Young, W., Wiggins, S., Limm, W., Fisher, C.M., Dejager, L., Genualdi, S., 2022. Analysis of per- and Poly(fluoroalkyl) substances (PFASs) in highly consumed seafood products from U.S. Markets. Journal of Agricultural and Food Chemistry 70 (42), 13545–13553. https://doi.org/10.1021/acs.jafc.2c04673.

Zarębska, M., Bajkacz, S., Hordyjewicz-Baran, Z., 2024. Assessment of legacy and emerging PFAS in the Oder River: occurrence, distribution, and sources. Environ. Res. 251, 118608. https://doi.org/10.1016/j.envres.2024.118608.

Zhang, J., Naveed, H., Chen, K., Chen, L., 2025. Toxicity of per- and Polyfluoroalkyl substances and their substitutes to terrestrial and aquatic invertebrates—a review. Toxics 13 (1). https://doi.org/10.3390/toxics13010047.

Zhang, X., Lohmann, R., Sunderland, E.M., 2019. Poly- and Perfluoroalkyl substances in seawater and plankton from the northwestern Atlantic margin. Environ. Sci. Technol. 53 (21), 12348–12356. https://doi.org/10.1021/acs.est.9b03230.

Zhao, P., Xia, X., Dong, J., Xia, N., Jiang, X., Li, Y., Zhu, Y., 2016. Short- and long-chain perfluoroalkyl substances in the water, suspended particulate matter, and surface sediment of a turbid river. Sci. Total Environ. 568, 57–65. https://doi.org/10.1016/j.scitotenv.2016.05.221.

Zhou, Z., Liang, Y., Shi, Y., Xu, L., Cai, Y., 2013. Occurrence and transport of perfluoroalkyl acids (PFAAs), including short-chain PFAAs in Tangxun Lake. China. Environmental Science and Technology 47 (16), 9249–9257. https://doi.org/10.1021/es402120y.